Carbon nanotube-based materials as capacitive deionization electrodes

Wang Xiaomei[1,2,*]

(1. *College of Materials and Chemical Engineering*, *ZiBo Polytechnic University*, *Zibo* 255000, *China*;
2. *College of Chemistry and Chemical Engineering*, *Ocean University of China*, *Qingdao* 266000, *China*)

Abstract: Capacitive deionization (CDI) is an emerging desalination technology that uses ion electrosorption at electrically charged electrode interfaces and has gained increasing recognition as a sustainable and cost-effective solution for water purification. Among the various electrode materials, carbon nanotube (CNT)-based structures have attracted considerable research interest because of their outstanding physicochemical properties, including high specific surface area, superior electrical conductivity, and excellent electrochemical stability. Significant efforts have been devoted to improving the CDI performance of CNT-based electrodes using material engineering and structural design. A comprehensive analysis of recent advances in performance optimization strategies for CNT-based CDI electrodes is provided, and their pivotal role in driving technological progress in CDI is evaluated. Persistent challenges and promising research to overcome current limitations are also considered.

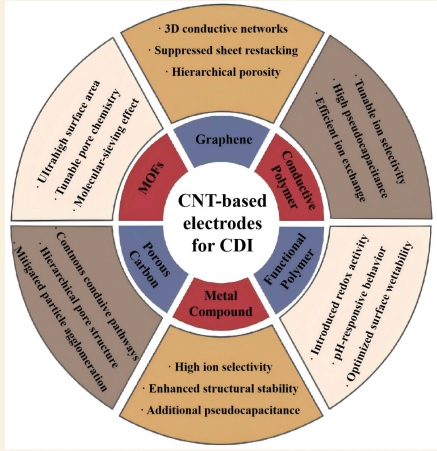

Key words: Carbon Nanotube; Electrosorption; Capacitive deionization; Desalination; Electrode materials

1 Introduction

As global demand for clean water continues to rise, natural freshwater resources are increasingly under pressure, and water scarcity has emerged as one of the key challenges of the 21st century[1–3]. Addressing this issue through the development of efficient water purification technologies, such as seawater and brackish water desalination, has become a research priority[4–5]. Various water treatment technologies have been explored to date, including reverse osmosis, electrodialysis, and thermal distillation. However, these conventional technologies are often associated with inherent limitations, such as high capital and operating costs, substantial energy consumption, and adverse environmental impacts, which hinder their large-scale deployment[6–8].

CDI is a comparatively new desalination process that removes dissolved salts from brackish water by electrosorption onto electrode surfaces when ions form electric double layers (Fig. 1a). The process has demonstrated considerable potential for producing drinking water from brackish water resources[9]. Similar to electric double-layer capacitors (EDLCs) used for energy storage, CDI devices are often referred to as flow-through capacitors, as they typically operate with brackish water continuously flowing through the cell[10–12]. Regeneration can be readily achieved when the electrodes become saturated with salt ions by reversing the applied potential or by short-circuiting the electrodes[13]. CDI offers several important advantages over conventional desalination methods, including the absence of chemical additives during operation and the application of low voltages, which helps avoid water electrolysis[14–15]. Thus, CDI represents a cost-effective and environmentally friendly alternat-

Received: July 22, 2025
Revised: November 09, 2025
Accepted: November 10, 2025

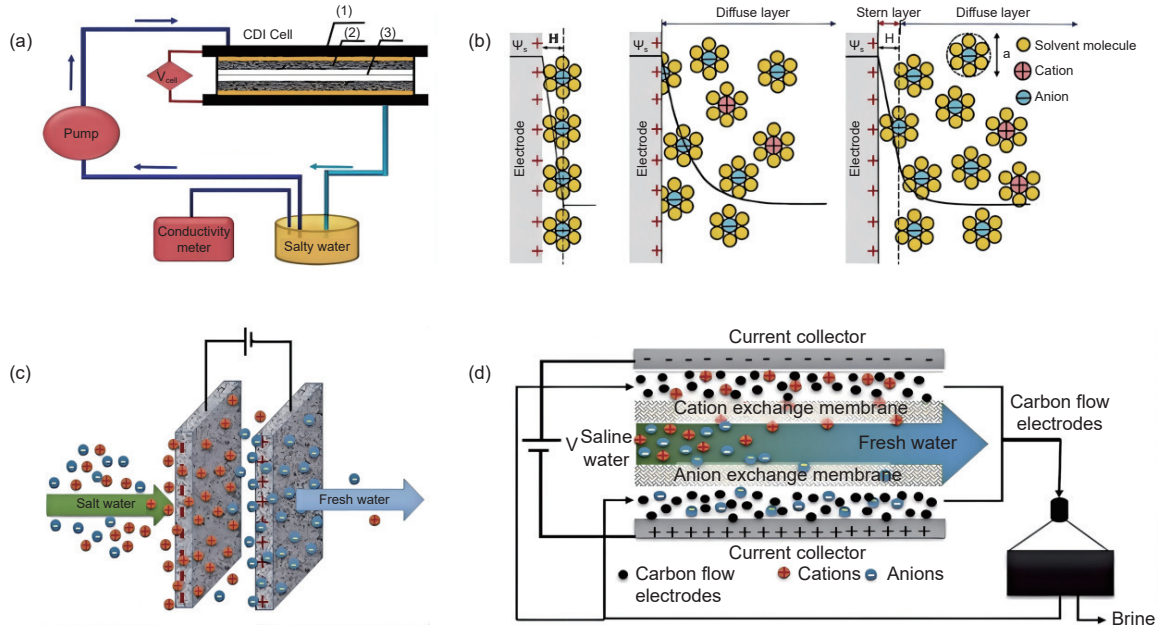

Fig. 1 (a) Schematic diagram of a typical CDI system. Copyright 2018, Elsevier. (b) Schematic diagram of how to create Electrical Double Layers, Copyright 2018, Elsevier. (c) A flow-through electrode (FTE) CDI System. Copyright 2018, Elsevier. (d) A flow electrode (FE) CDI System. Copyright 2018, Elsevier

ive to conventional desalination methods, such as thermal distillation, reverse osmosis, and electrodialysis[16–17]. This technology holds significant promise for providing affordable and pollution-free drinking and agricultural water. Previous reviews have categorized CDI as a replacement desalination technology, with membrane-based, flow-through, hybrid, and entropy battery systems classified as its major subcategories[18–20].

Ideal CDI electrode materials should possess the following characteristics: (1) a high specific surface area to provide abundant ion electrosorption sites; (2) a well-optimized pore size distribution, featuring high microporosity for enhanced salt electrosorption capacity along with an interconnected macroporous network for facile ion transport; (3) high electrical conductivity to ensure uniform voltage distribution across the electrodes and minimize resistive heat generation; (4) high wettability to promote effective contact between the electrode materials and ions, thereby maximizing pore utilization during the CDI process; and (5) excellent electrochemical stability, which is critical for the design of CDI electrodes capable of withstanding redox reactions and achieving long operational lifetimes[21–28]. Among various candidates, carbon nanotubes (CNTs) have attracted considerable attention as promising CDI electrode materials due to their unique structural, electrical, and chemical properties[29]. CNTs exhibit a large surface area, excellent electrical conductivity, and high mechanical stability, which are essential for ensuring high ion electrosorption capacity, efficient charge transfer, and long-term durability of CDI electrodes[30–31]. In addition, the tunable surface chemistry of CNTs enables functionalization and composite formation with other materials, thereby allowing precise tailoring of electrode properties to meet specific desalination requirements[32]. Recent advances have focused on integrating CNTs with other carbon materials, metal oxides, polymers and conductive hydrogels to further enhance CDI performance[33–35]. CNT-based composites often exhibit synergistic effects, such as improved wettability, enhanced ion selectivity, and superior stability during repeated charge-discharge cycles[36–37]. Furthermore, the utilization of CNTs-based electrodes in hybrid CDI systems, combining CDI with other desalination or energy storage technologies, has opened new avenues for achieving optimal energy efficiency and desalination capacity[38]. Despite these advances, several challenges remain. Issues including electrode fouling, scaling, and material aging during long-term operation must be addressed to enable the practical deployment of CDI

technologies. In addition, the current fabrication cost of high-quality CNTs remains relatively high, limiting their large-scale applications. These challenges call for the development of novel electrode architectures, scalable synthesis strategies, and next-generation CDI systems[39–41].

This review provides a comprehensive overview of the application of CNTs and their composites in capacitive deionization. It discusses the fundamental principles of CDI, the unique advantages of CNTs-based materials as electrode candidates, recent advances in material innovation and integration strategies, as well as the remaining challenges associated with large-scale deployment. By consolidating recent achievements and outlining future research directions, this work aims to contribute to the development of next-generation CDI technologies for sustainable and environmentally friendly water desalination.

2 History and theory of CDI

2.1 History of CDI

CDI is a relatively recent desalination technology compared to conventional desalination processes and was first conceived in the 1960s by Caudle and Hodes[42]. Early studies by Caudle et al. demonstrated the feasibility of using porous electrodes to remove ions from brackish water under an applied electrical potential, based on the principle of ion electrosorption at charged electrode surfaces. This pioneering work laid the foundation for subsequent investigations into CDI mechanisms and electrode materials[43–45].

In later years, Johnson and Newman further established the theoretical framework of CDI by proposing a porous electrode model[46–47]. Their model examined the interplay among ion electrosorption, electrical double-layer characteristics, electrode surface area, and applied voltage, providing deeper insights into ion storage behavior in porous carbon electrodes during the CDI process[48–50].

The breakthrough occurred in the 1990s when Farmer et al. prepared carbon aerogels with unusually high surface areas and conductivity[51]. These compounds significantly enhanced CDI performance by increasing ion storage capacity and efficiency. This breakthrough stimulated a vast amount of research on carbon-based materials, leading to innovations such as activated carbons, graphene, CNTs and carbide-derived carbons[52].

Over time, material technology has improved the performance of CDI systems considerably. High-surface-area materials and specifically engineered electrodes have enabled increased salt electrosorption capacities, making CDI not only feasible but also a more practical option for desalination and water treatment applications. CDI continues to be a viable and sustainable technology for addressing global water scarcity today[53–55].

2.2 Theory of CDI

CDI theory is primarily based on the concept of Electric Double Layer (EDL) that is formed at the interface of a charged electrode surface and an electrolyte solution[56]. The EDL accounts for the charge segregation caused by electrostatic forces that create two distinct charged layers: one immobile on the electrode surface and another mobile in the surrounding electrolyte[57].

Under the CDI conditions, an external voltage across electrodes causes cations and anions of the electrolyte to migrate to oppositely charged electrodes, where they are adsorbed and accommodated within the EDL. This process displaces ions from the electrolyte and efficiently desalts the solution[58–60].

2.2.1 Classic EDL theory

The classic EDL theory, initially proposed by Helmholtz, describes the EDL as a parallel-plate capacitor with a single layer of tightly packed ions attached to the electrode surface[61–62]. This theory does not account for the dynamic distribution of the ions within the electrolyte. Later developments by Gouy and Chapman introduced the concept of a diffuse layer, where the potential of electrolyte ions exhibits an exponential decay with distance from the electrode surface[63]. The Gouy-Chapman theory is closer to the ion distribution but overestimates capacitance, as it treats ions as point charges, leading to excessively

high charge densities[64–65].

In 1924, Stern combined the Helmholtz and Gouy-Chapman theories and presented a more refined description of the EDL[66]. The Stern model divides the EDL into 2 main regions. **Stern layer**: A thick layer of strongly adsorbed ions on the surface of the electrode. **Diffuse layer**: A region where the ions are loosely bonded and distributed in a Boltzmann distribution fashion. This two-layered structure accurately models the relationship between ion electrosorption and spatial charge distribution in an electrolyte[67–69].

2.2.2 CDI Mechanism and ion dynamics

In the CDI system, high-surface-area porous carbon materials are usually used for electrodes to facilitate EDL formation as much as possible[70–71]. When an potential difference is applied, the positive ions (cations) are attracted towards the negative electrode. Negatively charged ions or anions travel towards the positive electrode. They form the Stern layer near the surface of the electrode and a diffuse layer in the bulk electrolyte further away from the surface. Ion electrosorption reduces the concentration of ions to induce desalination[59,72].

CDI can be regenerated by discharging the electrodes, thereby releasing the adsorbed ions back into the solution. This regenerating capability renders CDI more energy-efficient compared with conventional desalination technologies, such as reverse osmosis. Ideally, the hydration shell contains excess ions that are electrostatically attracted and adsorbed at the vicinity of the Stern plane[73] (Fig. 1b). The parameter H represents the thickness of the Stern layer, corresponding to the Helmholtz double layer distance, while ψ denotes the electric potential at the electrode surface. Eq. (1) describes the decrease in ion concentration as a function of distance from the electrode surface, following the Boltzmann distribution with respect to electric potential and temperature.

$$C_{j,x} = C_{\text{bulk}} \times \text{EXP}(-Z_j \times \Phi(x)) \quad (1)$$

where $C_{j,x}$ is the concentration at electrode, C_{bulk} is bulk concentration, $\Phi(x)$ is the potential distribution with distance x from electrode divided by thermal voltage $(VT)^1$, and Z_j is ionic charge number.

In double layer theory, the potential at the Stern plane is determined by a key surface electrical property known as the zeta potential. This value is influenced by the chemical composition of the particle's surface and the pH of the solution in which the particles are dispersed[74].

The capacitance of a double layer is calculated by modeling it as 2 hypothetical capacitors connected in series, as expressed in Eq. (2):

$$\frac{1}{C_{\text{d1}}} = \frac{1}{C_{\text{st}}} + \frac{1}{C_d} \quad (2)$$

where C_{dl} is the total capacitance of double layer, C_{st} is stern layer capacitance and C_d is the Gouy-Chapman capacitance.

Eq. (3) estimates the Stern layer capacitance under the assumption of a fixed capacitance for symmetric ions, whereas Eq. (4) provides the calculation of C_d according to the Gouy-Chapman-Stern theory.

$$C_{\text{st}} = \frac{\varepsilon}{4\pi d} \quad (3)$$

$$C_d = \frac{\varepsilon}{\lambda_d} \times \cos h\left(\frac{Z \times \Delta\Phi_d}{2}\right) \quad (4)$$

where C_{st} represents the Stern capacitance, ε is the dielectric permittivity in C V^{-1} m^{-1}, d is the Stern layer thickness, $\Delta\Phi_d$ is dimensionless potential difference over diffuse layer1 and λ_d is the Debye length (m). According to Eq. (3), the Stern capacitance depends primarily on the thickness of the Stern layer, which is approximately equal to the hydrated radius of the ions. In contrast, Eq. (4) suggests that a reduction in the Debye length, achieved by increasing the electrolyte concentration, results in a higher capacitance[75–77].

2.3 Factors that influence CDI efficiency

The operation of a CDI cell is normally quantified by the electro-sorption capacity, and this will also be dominated primarily by most crucial factors such as cell design, electrode selection, operating process conditions, and water composition of the feed. All these thus need to be examined in great depth when developing a CDI system.

2.3.1 Structural geometry of a CDI cell

In experimental CDI cell design, both the feedwater flow direction and electrode configuration play critical roles in determining desalination

performance[78]. A typical CDI system consists of 2 porous carbon electrodes with thickness below 500 μm, arranged in parallel and separated by a narrow gap of approximately 0.6-1 mm to allow water to pass through. Based on the water flow configuration, CDI cells can be classified into flow-by (FB) or flow-through systems (Fig. 1c). The FB configuration is the most widely used arrangement in laboratory-scale studies[79–80]. In this configuration, saline water flows through the gap between 2 parallel porous carbon electrodes. The electrodes are typically fabricated as thin films or coated onto conductive substrates, such as graphite, copper, or titanium, which serve as current collectors.

Nevertheless, flow-by CDI systems face several challenges[81]. First, desalination in FB configurations is largely diffusion-controlled, resulting in relatively long processing times. Second, the separator positioned between the electrodes serves a dual function: enabling fluid transport while preventing electrical short circuits. Consequently, its thickness must be carefully optimized to minimize electrical resistance without compromising water flow efficiency[82–84].

The CDI cell geometries discussed above operate in a discontinuous manner with 2 distinct steps: electrosorption to remove ions and desorption to recharge the electrodes[85–86]. The second drawback of FB and flow-through electrode (FTE) CDI systems is the additional energy required for electrode regeneration. In an attempt to alleviate these, the flow electrode (FE) concept (Fig. 1d), explored by Micka in the 1960s, has been presented as a solution for the application of continuous CDI operation[87]. This configuration enables uniform concentration distribution in the split outlet stream.

In Fig. 1d, the FECDI process enables simultaneous regeneration and desalination of the electrode[18]. This is facilitated by passing a highly conductive carbon slurry in two distinct directions since ion exchange membranes that electrically insulate the electrodes from the feed stream prevent ion exchange between feed stream and electrodes[88]. The carbon slurry treated by the CDI system can subsequently be regenerated through mixing of the anodic and cathodic streams, which facilitates carbon particle separation and brine formation. In comparison with carbon particle saturation limiting FB and FTE CDI systems, FECDI regulates saturation through the adjustment of the slurry flow rate as well as electrode circulation channel diameters[28,85,89].

2.3.2 Feedwater characteristics

The composition of the feed water plays a critical role in determining the performance of CDI systems[86,90]. It significantly influences key performance metrics, including ion removal efficiency, energy consumption, and electrode stability. Feed water composition varies depending on the source and may contain a wide range of ionic species, organic compounds, and other contaminants. The interactions between these constituents and CDI electrodes are therefore crucial for understanding desalination mechanisms and for optimizing system performance[91–93].

The concentration and speciation of ions in the feed water are critical factors that affect how well the CDI works. For instance, monovalent ions such as sodium (Na^+) and chloride (Cl^-) are more likely to be removed. This is because they have smaller hydration radii, and they are more mobile than divalent ions or multivalent ions like magnesium (Mg^{2+}), calcium (Ca^{2+}), or sulfate (SO_4^{2-})[94]. High concentrations of salt can increase the competition among ions for the electrosorption sites that are present on the electrodes[95]. This increased competition may reduce the system's ion removal capacity. At the same time, when the ionic strength goes up, it may cause the thickness of the EDL to decrease. A smaller EDL thickness might change the way the electrosorption mechanism works, possibly affecting energy efficiency in ways not fully understood. The effects of these factors can vary, and their relationship to the overall performance of the system is not always straightforward[96–98].

2.3.3 Operating conditions

Temperature and flow rate primarily affect ion electrosorption on electrode surfaces in CDI[86,99]. The temperature will control the ionic mobility as well as

the ionic diffusion rate, and the greater the rise in temperature, the greater the ion movement as well as the ion removal rate[100–101]. Although increasing temperature enhances ionic mobility, it can decrease electrostatic interactions between the electrode surface and ions and lower electrosorption capacity. A suitable temperature is thus essential in delivering greater ion transport and stable electrosorption[102–103].

Flowrate, which decides ions' residence time in the electrode gap, is also an important parameter for CDI performance[78,104–105]. High flowrates reduce residence time of ions close to electrodes and thus limit electrosorption efficiency. Low flowrates enhance residence time and thus achieve maximum ion-electrode interaction and electrosorption. Very low flowrates can, however, reduce the system throughput and thus overall efficiency[106].

Apart from flowrate and temperature, pH value is also an important parameter in CDI performance[107]. The pH of the feedwater affects the ionization of the various ions and the surface charge of the electrode. Decreased pH increases the concentration of protons (H^+), which can lead to a more positive electrode surface charge that would enhance anion electrosorption[108]. On the other hand, at high pH values, hydroxide ion concentration (OH^-) is higher and thus increases the negative electrode surface charge, which favors cation electrosorption. pH also influences the electrochemical stability of electrodes since extreme alkalinity or acidity can cause electrode breakdown or corrosion and thus decrease the efficiency and lifetime of the system[81]. Additionally, the ion selectivity of CDI systems is also influenced considerably by the solution pH. Electrostatic attraction towards the surface of the electrode and towards anions is stronger in acidic pH, whereas with cations it is stronger in alkaline pH[109–111]. Hence, pH conditioning of the feed water can be a method of optimizing in removal of target ions depending on what type of contaminants are present in the water.

2.3.4 Electrical potential

Because CDI is driven by an applied electrical potential, this parameter plays a dominant role in regulating the electrosorption-desorption process and, consequently, the overall desalination efficiency[112–113]. Increasing the applied potential strengthens the electrostatic attraction between the electrode surface and ions, thereby enhancing the electrosorption capacity. However, excessively high potentials may induce undesirable effects, such as electrode polarization, overcharging, and parasitic side reactions, which can compromise desalination performance and lead to progressive electrode degradation over prolonged operation[109].

The electrical potential is also responsible for controlling the selectivity of ion removal because individual ions may have greater affinity with the electrodes within certain ranges of potential[114–115]. Such selectivity proves to be beneficial for selective elimination of desalination or individual contaminants. The energy efficiency of CDI systems is similarly influenced by the potential applied; while increased potentials enhance ion removal, they use more energy. Optimal potential thus becomes the key to balancing efficiency and energy consumption[116–117].

During operation, the potential facilitates the migration of ions to oppositely charged electrodes during electrosorption and drives their release upon desorption, thus enabling regeneration of the electrodes. This mechanism emphasizes the importance of potential control in sustaining CDI performance[118]. Electrical potential in aqueous environments needs to be carefully controlled in order to achieve maximum desalination efficiency, electrode stability, and power usage, thus qualifying it as a key parameter in CDI operations.

2.3.5 Properties of electrode materials

The preceding discussions suggest that the structural and morphological properties of electrode materials play a crucial role in the performance of CDI systems. In particular, these properties support the development of a porous architecture that enhances ion electrosorption. This section examines the key characteristics that influence how electrode materials function across different CDI setups, from commercially available activated carbons to advanced hybrid composites that incorporate metal oxides, polymers, and

carbon nanomaterials.

It is important to note that the effectiveness of these materials depends not only on pore structure, but also on a range of other factors. These include electrochemical stability, electrical conductivity, surface chemistry, wettability, mechanical strength, and cost-effectiveness[114,119]. A comprehensive understanding of how these properties interact is essential for designing efficient and practical CDI systems.

To achieve optimal CDI performance, several key material properties must be taken into account. A high specific surface area (SSA) is crucial because it offers ample active sites for ion adsorption. However, not all of the measured surface area is necessarily accessible to ions, making the electrochemically active surface area a more relevant metric. Although micropores (< 2 nm) greatly contribute to SSA and support charge storage through electrical double-layer formation, they can also impose steric limitations that hinder the movement of ions, especially those with larger hydration shells[120–121]. In comparison, mesopores (2-50 nm) act as conduits for ion transport, lowering diffusion resistance and enhancing reaction kinetics, though often at the expense of volumetric capacitance. Macropores (> 50 nm), meanwhile, promote bulk electrolyte flow. Thus, an optimal electrode should possess a hierarchical pore network that intelligently balances micro-, meso-, and macropores to improve both ion access and storage capability[122].

Electrical conductivity is equally vital, as it promotes uniform charge distribution across the electrode and reduces energy losses and Joule heating during operation. Highly conductive materials support faster electron transfer, which is necessary for achieving high-rate performance and energy-efficient desalination[123]. Moreover, electrodes must exhibit strong electrochemical resilience under varying voltage and pH conditions to maintain performance over repeated cycling. Chemical and mechanical durability are also key to avoiding corrosion, deformation, or structural failure, thereby supporting long-term operational reliability[112].

Wettability is another fundamental aspect governing the electrode-electrolyte interface. Hydrophilic surfaces improve electrolyte permeation and help fully utilize the porous interior, which in turn boosts electro-adsorption capacity and kinetics. On the other hand, hydrophobic surfaces may result in inadequate wetting and diminished effectiveness. Accordingly, surface modifications such as chemical functionalization or composite integration are commonly used to optimize wetting behavior[124–126].

Finally, cost and scalability play decisive roles in the real-world adoption of CDI systems. Although advanced nanomaterials often show improved performance, their expensive and complex production processes may limit widespread use. This has spurred interest in developing electrode materials that are not only efficient and durable but also economically viable and scalable[127].

Common carbon-based materials used in CDI include activated carbons (ACs), activated carbon fibers (ACFs), carbon aerogels, templated carbons, CNTs, carbon nanofibers (CNFs), and graphene. Of these, CNT-based electrodes have attracted notable interest due to their high surface area, exceptional electrical conductivity, mechanical strength, and ease of functionalization. The following section discusses in greater detail the role of CNT-based materials in CDI applications[101,128].

3 CNT-based electrode materials in CDI

From the above discussed points, it can be concluded that the electrode material has an effective role in optimizing the performance of CDI systems, where intense focus has been laid on electroconductivity, structural durability, and low costs. Out of many electrode materials screened, CNTs have gained considerable attention due to their unique physicochemical characteristics, as well as their potentialities towards enhanced CDI performance[129–130]. Application of CNTs as electrode material in CDI technology exploits their large surface area, high electrical conductivity, and chemical stability.

The pore structure of CNT-based electrodes

plays a decisive role in ion electrosorption, and optimal design requires a well-balanced distribution of micropores and mesopores. Mesopores serve as ion transport channels, while micropores have active sites with rich resources for electrosorption of ions[131]. The interface between these 2 pore regimes offers flexibility in achieving high ion mobility and efficient surface area utilization, which are essential for high-performance CDI applications. Moreover, the high electrical conductivity of CNTs ensures efficient charge distribution with minimum energy loss and reduced thermal effects during operation[132–133].

The hydrophilic functionalization of CNTs can enhance their wettability, ensuring all active surface areas are engaged in the CDI process. Moreover, the chemical inertness and mechanical stability of CNTs under various conditions of pH as well as voltages enable operation cycles for a long period without time-dependent material degradation. Furthermore, the economic feasibility and scale-up possibility of CNT-based electrodes also potentially increase the practice-based application of CDI systems[134–135].

Various CNT-based configurations including pristine CNTs, CNTs composites, and hybrid materials incorporating metal oxides or polymers have been used to optimize CDI performance[136]. Different kinds of CNT-based electrodes and their ways to increase the application and efficiency of capacitive deionization are presented in the following sections.

3.1 Pristine and modified CNT electrodes

CNTs have the potential to become electrode materials in CDI application due to their high electrical conductivity, huge specific surface area, and superior chemical stability. However, there are 2 primary challenges that prevent the use of CNTs as CDI electrodes. One, CNTs are naturally hydrophobic, resulting in an undesirable electrode-water interface in the desalination process[137]. This hydrophobicity also promotes aggregation in water, reducing the effective surface area for ion removal. Additionally, use of CNTs with binders or additives significantly deteriorates their properties, reducing the efficiency and reaction kinetics of CDI[138]. Second, processing and immobilization of CNTs have a tendency to alter their porosity, preventing the capacitance from reaching its theoretical limit[139]. Therefore, CDI electrode design requires a mechanically robust, scalable, and stable substrate with optimized porosity for immobilization and nanocarbon accommodation[140]. Cellulose yarns with biocompatibility were successfully developed by Moronshing et al. as favorable substrates for the anchoring of CNTs (Fig. 2a)[141]. The native porosity as well as the hydrophilicity of cellulose synergistically enhances the performance of CNTs in CDI processes. Moreover, the CNT-immobilized yarns are scalable and can be utilized in numerous structural formats, which makes them particularly promising for a variety of applications. The CNTs electrodes prepared have an electro-sorption capacity of 139 mg g^{-1} and a salt electrosorption rate of 2.78 mg g^{-1} min^{-1}. In addition, the system exhibited efficient removal (~ 80%) for cations (Na^+, K^+, Mg^{2+} and Ca^{2+}) and anions (Cl^-, SO_4^{2-} and NO^{3-}). With a tunable capacitance of 0.4–120 mF and a high specific capacitance of ~ 27.2 F g^{-1}, the device exhibits superior performance in a broad range of saline concentrations (50-1000 mg L^{-1}). After 5 cycles, the performance degradation is less than 3%, indicating that the electrode material exhibits excellent cycling stability.

In recent years, nitrogen doping in carbon materials has garnered significant attention due to its enhancement of electrochemical activity[142]. Electrical conductivity, wettability of carbon structures, and ion electrosorption capacity are enhanced with nitrogen doping[143]. Following the trailblazing study on nitrogen-doped graphene for CDI purposes, many kinds of nitrogen-dense carbon materials with variable morphology have been produced[144]. Of these, CNTs have shown remarkable performance in a wide range of electrochemical applications because of their increased electrode-electrolyte contact and reduced ion and electron diffusion distances. Despite having all these benefits, the synthesis of nitrogen-doped CNTs for particular CDI applications is still a serious challenge[145]. In an attempt to overcome this challenge, Shi et al. synthesized nitrogen-doped CNTs (nit-

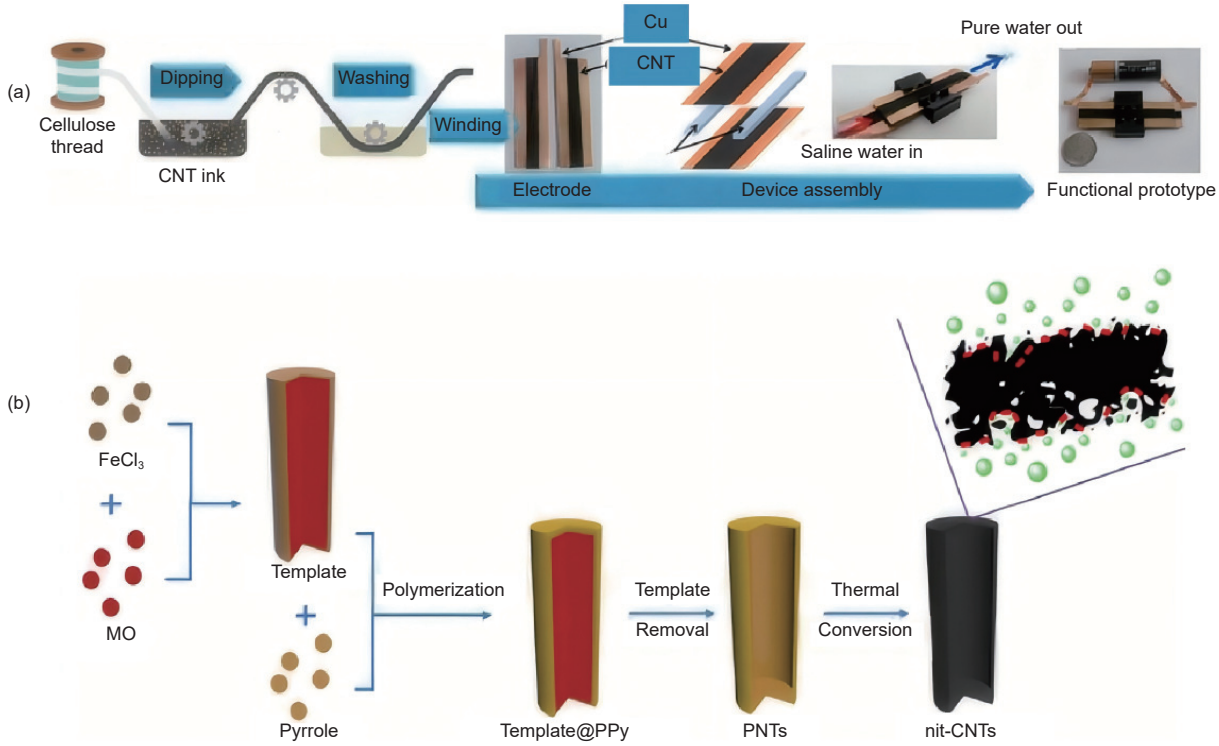

Fig. 2 Schematic illustration displaying the preparation process: (a) Fabrication of electrode and its assembly to form the final functional prototype[141]. Copyright 2017, American Chemical Society. (b) Schemes for the synthetic procedure of nit-CNTs[146]. Copyright 2019, Elsevier

CNTs) through thermal conversion of polypyrrole nanotubes in a nitrogen atmosphere (Fig. 2b)[146]. Compared with commercially purchased CNTs synthesized by the chemical vapor deposition method, the nit-CNTs synthesized have some outstanding merits: (1) 3D network structure of nanotubes, which offers enough space for ion storage and excellent paths for electron transmission. (2) Abundant nitrogen dopants within the carbon lattice, which leads to high electrical conductivity and ion electrosorption. (3) Open tube walls, which enhances the electrosorption ability of ions further. Thereafter, the nit-CNTs possess a capacity of up to 17.18 mg g^{-1} for desalination and also exhibit excellent cycling stability with hardly any loss of capacity after 20 cycles.

Major challenges in applying CNTs as CDI electrodes include their high energy requirements and dependence on binders for flat-sheet fabrication. Currently, the application of CNT electrodes is primarily limited to doping or blending with support materials[147]. The intrinsic hydrophobicity of CNTs impedes both ion transport and electrosorption in seawater, and therefore hydrophilic modification is necessary for enhanced performance as CDI electrode materials[114]. Common hydrophilization methods, such as strong acid treatment, enhance electrosorption capacity. Moreover, grafting hydrophilic functional groups such as sulfonic acid and amine onto pretreated CNTs surfaces can significantly improve surface wettability[148]. However, these treatments introduce additional processing steps, complicating the overall preparation process[41]. Lee et al. successfully fabricated electrically conductive free-standing hollow fiber CNTs (HF-CNTs) using wet-spinning technology[149]. Wet-spinning is a fiber-forming technique where a CNT dispersion is extruded through a spinneret into a coagulation bath, forming hollow fiber structures without electrical field application. After the removal of the binding polymers, HF-CNTs retain the excellent electrical properties of CNTs but exhibit better water wettability due to their three-dimensional hollow fiber structure that is more effective than 2D flat-sheet types. Thus, HF-CNTs have been utilized as CDI electrode materials with enhanced electrical performance and remarkable electrosorption capacity based on their structural advantages. The HF-CNTs

exhibited a surface area of 55.6 m^2 g^{-1}, and the specific capacitance was 23.8 F g^{-1}, exhibiting excellent electrical stability under repeated current-voltage cycling. Consequently, the HF-CNTs electrode exhibited great electrosorption capacity of 58.2 mg g^{-1} in a 500 mg L^{-1} NaCl solution at a specific voltage of 1.2 V. The outstanding electrochemical characteristics of the HF-CNTs are attributed to their unique structure that reduces resistance for ion transfer and enhances electrosorption efficiency. The test results exhibited the outstanding retention of specific capacitance after 50 sweeps of potential, indicating good cyclic stability.

3.2 CNT/graphene composite electrodes

Carbon nanomaterials are widely investigated as electrode materials for CDI applications. However, despite their promising properties of high specific surface area and excellent electrical conductivity, graphene and CNTs have shown poor performance as CDI electrodes[150]. Such poor performance is largely due to the re-stacking of graphene sheets or bundles of CNTs caused by the strong π-π interactions, significantly reducing the effective surface area for ion electrosorption and storage[151].

Prominently, CNT/graphene hybrid composites have shown much greater capacitance and desalination efficiency. This is attributed to the better dispersion and prevention of re-stacking of the 2 components. Composites of graphene and CNTs are routinely prepared by the physical mixture of the 2 materials. Although this method is easy and effective, the homogeneous dispersion of the 2 components remains challenging. Wang et al. reported a chemical vapor deposition method to produce CNT/graphene composites in gram scale (Fig. 3a)[152]. The composite exhibited specific capacitance of 242.3 F g^{-1} at 0.5 A g^{-1}, more than four times that of pristine CNTs. Furthermore, the composite-based electrodes also showed excellent cycling stability with performance maintained over 4000 cycles at 1 A g^{-1}. This remarkable stability was due to their improved electrical conductivity and unique structural features. The composite, as an electrode in membrane capacitive desalination, achieved a

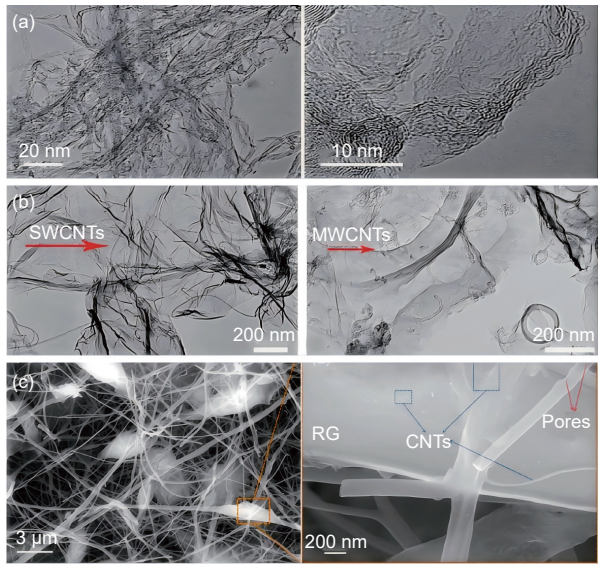

Fig. 3 (a) TEM images of as-synthesized CNT/graphene composites, Copyright 2021, Elsevier. (b) SEM images of CNT/graphene hybrid fiber, Copyright 2016, Elsevier. (c) SEM images of CNT/rGO hybrid fiber, Copyright 2018, Desalination

desalination capacity of 16.46 mg g^{-1} at 1.2 V applied voltage with 500 mg L^{-1} NaCl solution as feed water.

2D graphene suffers from several limitations in practical applications, including strong π-π interactions that induce sheet agglomeration, difficulties in electrode fabrication, and performance degradation arising from the use of polymer binders[153]. In contrast, 3D graphene gels offer distinct advantages over their 2D counterparts: First, their interconnected porous architecture provides abundant sites for ion accumulation and facilitates efficient ion transport, thereby enhancing electrosorption capacity. Second, 3D graphene gels exhibit macroscopic integrity and superior mechanical strengths, enabling their direct use as electrodes while mitigating issues such as pore blockage caused by binders[154–155]. Among various 3D graphene-based materials, graphene hydrogels (GH) have been popularly utilized as CDI electrode materials. However, their modest electrosorption speed and conductivity limit the electrosorption performance of GH, representing the necessity for improvement[156–157]. The combination of CNTs with graphene has then been discovered to be an effective means to enhance the electrosorption capacity of GH. The incorporated CNTs function as conductive networks and suppress graphene sheet agglomeration.

Cao et al. developed a one-step water bath method to prepare 3D graphene hydrogels with CNTs to promote material conductivity and suppress graphene sheet agglomeration (Fig. 3b)[158]. The experiments indicated that CNT/graphene possessed an electrosorption capacity of 48.73 mg g^{-1} owing to its large specific surface area (308.37 m^2 g^{-1}) and specific capacitance (36.35 F g^{-1}). These results indicate CNT/graphene as a highly compatible and prospective material for CDI applications.

The industrial application of CNT/graphene composites in CDI is primarily limited by prohibitively high production costs and the complexity of synthesis protocols. Although the materials are blessed with excellent properties such as excellent electrical conductivity, enormous surface area, and excellent chemical stability, the complex synthesis processes often require expensive precursors, advanced equipment, and energy-intensive protocols[159]. Furthermore, scalability is also a hurdle that hinders their widespread application in CDI technology, particularly industrial-scale applications. To satisfy these requirements is the development of cost-effective and efficient fabrication techniques to bridge the gap between commercialization and laboratory development[160–161]. Luo et al. developed CNTs composites incorporating reduced graphene oxide (rGO) through electrospinning and subsequent heat treatment, with potential for large-scale production (Fig. 3c)[162]. Microstructural characterization revealed that the CNTs became embedded within the inner fiber matrix and intercalated between graphene layers, thereby generating additional defects and pores that significantly enhanced electrosorption performance. The as-prepared tri-component nanofibers could be directly used without binders, demonstrated a desalination capacity of 13.6 mg g^{-1} for a 500 mg L^{-1} NaCl solution and also demonstrated excellent cycling stability and 98% capacitance retention after 1000 charge-discharge cycles. The incorporation of GO and CNTs significantly enhanced conductivity and electrosorption efficiency. The tri-component CNTs sheet has high potential in the fabrication of high-performance electrodes for different CDI applications.

3.3 CNT-conductive polymer composite electrodes

Conductive polymers serve as pivotal electrode materials in CDI systems, demonstrating exceptional deionization capabilities through their unique doping/dedoping mechanisms and ion-exchange properties[163]. The hybrid materials formed by integrating conductive polymers with CNTs are considered ideal electrode systems for efficient electrosorption, synergistically combining the high pseudocapacitance of conductive polymers with the superior electrical conductivity of CNTs[164].

3.3.1 CNT-based polypyrrole electrodes

Polypyrrole (PPy) has attracted considerable research interest in CDI applications owing to its outstanding electrochemical properties, including high electrical conductivity, substantial surface area, and excellent ion exchange capacity. The internal conductivity of PPy, along with its facile doping/dedoping process, enables efficient and rapid electrosorption of ions during the CDI process[165]. PPy's ability to undergo electrochemical and structural changes also enhances performance, since it can be precisely tuned as far as ion-selective qualities. All these traits make PPy an extremely potential player in enhancing efficiency and sustainability within CDI technology, specifically where ion removal ability and energy are concerned[166].

Despite its advantages, PPy faces limitations in CDI applications primarily due to its inherent electrochemical instability. Furthermore, the incorporation of polymeric binders during electrode fabrication negatively impacts both the electrical conductivity and electrosorption performance of the material[167]. Scholars began looking for some solutions in order to transcend these issues. Current studies have revealed that the synergistic action between PPy and chitosan is largely responsible for PPy stability and this is a result of chitosan functional groups $-NH_2$ and $-COOH$. Chitosan is also an excellent adhesive as a result of its very high viscosity and unique molecular structure[168–169]. Moreover, chitosan possesses higher

electrosorption capability in removing heavy metals, acidic ions, dyes, and other forms of contaminants. These good properties render the chitosan-PPy composite as a promising material for CDI electrode use. Zhang et al. prepared a PPy/CNT composite nanoelectrode by in situ polymerization (Fig. 4a)[170]. The specific capacitance and electrosorption capacity of the composite nanoelectrode were found to rise with increasing dosage of chitosan from the cyclic voltammetry measurements, before reaching plateau. The highest values achieved were 103.19 F g^{-1} and 16.83 mg g^{-1}, respectively. Specific capacitance reduced 13.1% at 100 cycles and the loss in the first 50 cycles and remaining 50 cycles was 9.7% and 3.4%, respectively. The above result verifies that composite electrode is extremely stable after 50 cycles. The electrosorption rate of the PPy/CS/CNT composite nanoelectrode at 100 mg/L concentration of $CuSO_4$ is 80.08%, which verifies the strong adsorbing capacity.

In composite electrode materials, ion doping is a strong method to enhance the capacitive deionization performance[171]. The dopant species in CNT/PPy composites modulate the electrode's ion-exchange properties, facilitating co-ion expulsion during charging while preventing counterion re-adsorption during discharging. The selection of dopants is critical in determining the ion exchange characteristics of the CNT/PPy composite electrode[172]. Various dopants may alter the electrochemical characteristics of the composite, making it perform better during charge/discharge cycles. Specifically, the dopants help remove co-ions easily from the electrode surface on charging. This leads to better ion mobility and an effective charging process[173]. The dopants also help prevent re-electrosorption of ions upon discharging and thereby ensure greater overall efficiency and stability of the electrode material through multiple cycles. The forms of the dopant must be optimized in order to enhance the performance and stability of energy storage systems using such composite electrodes[167]. Ma et al. successfully fabricated 2 types of composite electrodes for the CDI cell using chloride (Cl^-) and dodecyl benzene sulfonate (DBS^-) doped CNT/PPy[174]. The CNT/PPy-Cl electrode exhibits anion exchange characteristics, where facile Cl^- de-doping generates vacant positive sites on the PPy chain. In contrast, the CNT/PPy-DBS electrode adsorbs cations during charging, as the electronegativity of DBS^- permits electrosorption, while the bulky DBS^- is less prone to de-doping from the polymer chain. Further studies have concluded that the optimal CDI cell configuration consists of the CNT/PPy-Cl elec-

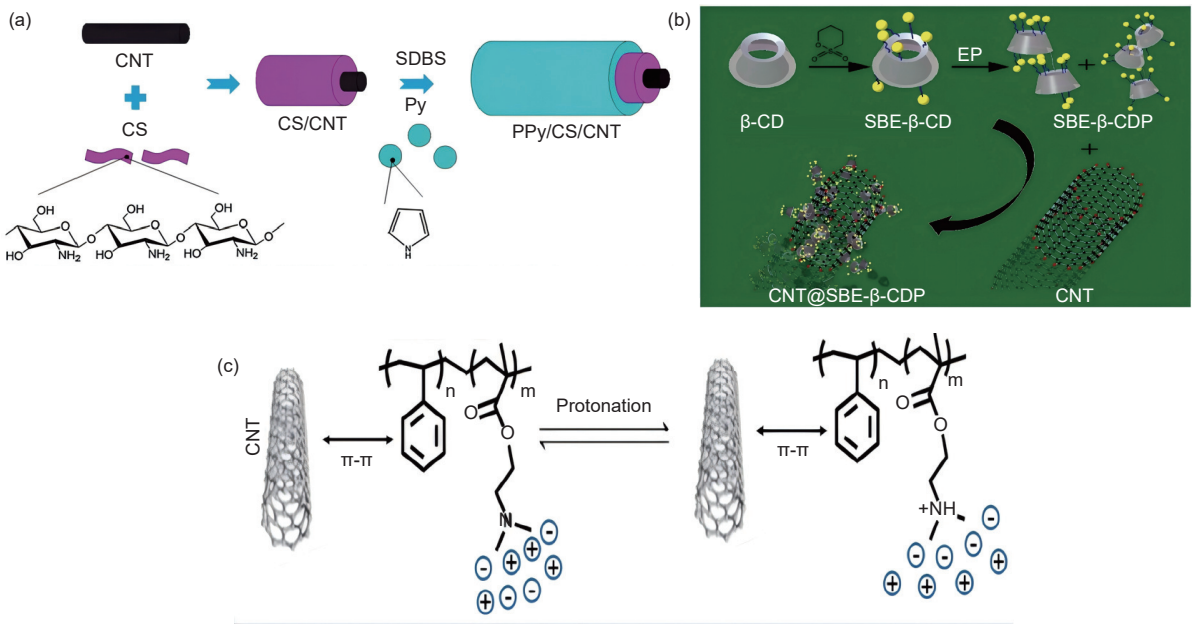

Fig. 4 (a) The preparation of PPy/CNT composite material. Copyright 2019, Elsevier. (b) Fabrication of the CNT/SBE-β-CDP. Copyright 2019, Elsevier. (c) Schemes for the synthetic procedure of CNT/PDMAEMA-b-PS. Copyright 2021, Elsevier

trode as an anode and the CNT/PPy-DBS electrode as a cathode. This configuration exhibits nearly double the saturated electrosorption capacity of the reverse configuration. These findings are the foundation for further studies on employing CNT/PPy electrodes. The electrode material possesses a maximum electrosorption capacity of 35.46 mg g^{-1} for sodium chloride, reflecting its strong ion removal capability. Moreover, after 20 consecutive charge-discharge cycles, the electrosorption capacity of the CNT/PPy-Cl and CNT/PPy-DBS assembled electrodes only suffered a degradation rate of 8.85%, reflecting superior cycling stability. This relatively low capacity loss is reflective of the high structural integrity and electrochemical stability of the composite electrodes, which makes them good candidates for long-term capacitive deionization applications.

3.3.2 CNT-based polyaniline electrodes

Polyaniline (PANI) and CNTs composites possess superior advantages in CDI applications based on their synergistic properties[175]. PANI, a conductive polymer that can be readily prepared, possesses high pseudocapacitance, which allows for greater charge storage and rapid ion electrosorption[176]. Upon combination with CNTs, the composite possesses enhanced ion removal efficiency, rapid charge-discharge cycles, and excellent long-term stability. Additionally, the hierarchical architecture of the composite improves accessibility of ions and therefore CDI efficiency, particularly in energy terms and ion selectivity during desalination[177]. The outstanding properties of CNT/PANI composites render them exceedingly promising for future water treatment technologies.

Compared to metal ion removal, an exhaustive literature survey reveals the exceptional prospect of CNT/PANI composite electrode materials in the selective removal of phosphate anions in CDI applications. CNTs show promise as CDI electrodes but exhibit limited phosphate storage capacity, low selectivity, and poor performance in wastewater with low phosphate concentrations[178]. The amino and imine functional groups in PANI have the ability to interact specifically with negatively charged phosphate anions (PO_4^{3-}) by electrostatic attraction or hydrogen bonding, thus facilitating the selective electrosorption of phosphate[179]. As a result, the CNT/PANI composite is an extremely promising electrode material with great environmental adaptability and excellent capacity for the selective capture of PO_4^{3-}. Zhang et al. developed a CNT-based electrode material through a simple co-precipitation method, incorporating polyaniline-doped carboxyl-intercalated metal hydroxide composites for enhanced phosphate removal from wastewater[164]. The results show that the CNT/PANI electrode exhibits efficient phosphate removal in 2–10 mg L^{-1} concentrations, largely attributable to electric double-layer capacitive electrosorption and pseudocapacitive electrosorption mechanisms. Notably, the effluent phosphate concentration was reduced to 0.095 mg L^{-1}. After 10 cycles, the phosphate removal efficiency remains above 77%, demonstrating excellent cyclic stability.

3.4 CNT-functional polymer modified electrodes

Polymer-functionalized CNTs possess particular advantages as electrode materials for CDI applications[180]. The functional groups (such as amino, carboxyl) grafted on the surface of CNTs enhance the hydrophilicity and electrochemical activity of CNTs, enhancing electrode-ion interactions and consequently improving electrosorption capacity. Furthermore, the functional polymers can modulate the electronic conductivity and mechanical stability of CNTs for long-term performance and structural integrity over numerous cycles[181]. The polymer treatment also allows for fine-tuning of the structural properties of the CNTs, such as porosity and specific surface area, which are ideal for charge storage and ion transport in the deionization process. Collectively, these qualities enable functional polymer-treated CNTs to realize improved performance in CDI systems and make them an attractive material for efficient and sustainable water treatment[182].

3.4.1 Hydrophilic polymer-functionalized CNT electrodes

Hydrophilicity enhances ion transport and electrode wettability, improving the efficiency and stability of CNT electrodes in CDI processes. It facilitates

better access of the electrolyte to the electrode surface, improving charge storage capacity and desalination performance[183]. In CDI processes, CNTs are usually oxidized to reverse their inherent hydrophobicity. However, this process has a tendency to yield suboptimal results. Researchers have employed advanced hydrophilic polymer modifications to enhance CNT hydrophilicity and CDI performance[184]. Ma et al. synthesized a novel sulfo-butyl ether β-cyclodextrin polymer (SBE-β-CDP) containing multiple hydroxyl and sulfonic groups as an electrode material modifier for CNTs (Fig. 4b)[185]. SBE-β-CDP, being a new charged polymer, exhibits excellent water solubility and ion selectivity. These properties originate from SBE-β-CD polymerization, with each molecule containing ~ 14 hydroxyl and 7 sulfonic groups. Depositing SBE-β-CDP onto carbon materials with non-covalent bonds is most likely to significantly alter the carbon electrode surface properties through a synergistic effect of the large numbers of hydroxyl and sulfonic groups. Additionally, the long-chain molecule structure of SBE-β-CDP helps alleviate self-aggregation of carbon materials, particularly CNTs. The as-prepared CNT/SBE-β-CDP electrode demonstrates significant enhancements in both capacitive performance and hydrophilicity compared to the pristine CNT electrode, reaching 60.9 F g^{-1} and 65.5°, respectively. Such an enhancement signifies that multisulfonic and hydroxyl groups on the surface of the CNT/SBE-β-CDP electrode promote efficient ion transmission through a synergistic effect. In desalination experiments, the average salt electrosorption capacity was 6.37 mg g^{-1}. Even after 50 cycles of experiment, the attenuation rate of salt electrosorption capacity was 4.4%, which indicates that the electrode material prepared is of excellent long-term stability.

3.4.2 Redox-active polymer-functionalized CNT electrodes

The modification of CNTs with redox-active materials is now widely recognized as an effective strategy to improve their performance in CDI. Numerous studies have investigated different redox-active materials for CDI applications, such as quinones, vanadium compounds, Prussian blue analogs, and iodide redox couples[186]. Despite this progress, these modified materials and composites face significant challenges. Their synthesis typically demands considerable time and effort. For instance, preparing quinone-modified CNTs requires 48 to 72 h of reaction time using solvent thermal processes. Similarly, vanadium compound composites need protection with an inert atmosphere like argon during high-temperature fabrication at 1000 °C or above to prevent oxidation, which substantially increases production complexity[21,186–187]. Another concern is that some additives, including quinones, show cytotoxic effects. With a half-maximal inhibitory concentration ranging from 0.1 to 1 μmol L^{-1} for aquatic organisms, these substances could potentially leak into freshwater systems, threatening both aquatic ecosystems and human health[188].

In response to these limitations, researchers have developed redox-active polymer modifications for CNTs as a promising alternative. This approach provides several key benefits that help overcome the drawbacks of conventional redox materials[189]. Redox-active polymers introduce additional faradaic charge storage mechanisms that work alongside the inherent electric double-layer capacitance of CNTs, leading to increased overall desalination capacity. The redox behavior of these polymers can be tuned through molecular design, for example by adjusting redox potentials, which enhances both energy efficiency and ion selectivity. Furthermore, polymer modification improves CNT wettability and dispersion. Compared to pristine CNTs, the aggregate size is reduced by 50% to 60%, resulting in better electrode utilization and improved electrolyte access.

Rauer and colleagues successfully functionalized CNTs with the redox-active polymer poly(3,4-ethylenedioxythiophene) polystyrene sulfonate (PEDOT:PSS) for CDI applications. In this system, PEDOT:PSS stores charge through reversible redox reactions involving the oxidation of thiophene units in PEDOT, while the sulfonate groups from PSS improve wettability and ion affinity. The resulting

PEDOT:PSS/CNT electrodes delivered exceptional CDI performance. When tested in a high-salinity brine containing 60 000 mg L^{-1} NaCl at an applied voltage of 1.2 V, these electrodes achieved a sodium chloride electrosorption capacity of 955 mg g^{-1}. This value is 10 to 20 times greater than that of pristine CNTs, which typically achieve 40 to 50 mg g^{-1}, and 5 to 8 times higher than quinone-modified CNTs, which reach 120 to 150 mg g^{-1}. The electrodes also showed outstanding cycling stability, maintaining 85% of their initial capacitance after 300 charge-discharge cycles at a current density of 1 A g^{-1}, demonstrating their potential for long-term reliable operation[190].

3.4.3 pH-responsive polymer-functionalized CNT electrodes

CNTs functionalized with pH-responsive copolymers offer distinct advantages in CDI systems due to their capacity to dynamically alter surface characteristics in response to changes in solution pH[191]. This copolymer modification improves the ion selectivity of CNTs, allowing the electrode to adsorb or reject specific ions depending on pH conditions. For example, it can preferentially capture anions in acidic environments and cations under alkaline conditions[192]. This adaptive capability enhances ion removal efficiency, making it particularly valuable for treating water sources with inconsistent composition, such as industrial wastewater with varying pH levels. Additionally, pH-responsive copolymers improve CNT wettability, reducing the water contact angle from over 100° to between 50° and 60°. They also create a protective film that reduces organic fouling by 40% to 50% by resisting humic acid adsorption, while simultaneously minimizing surface degradation to ensure long-term electrode durability[193–194]. The combination of CNTs' high electrical conductivity and mechanical strength with the pH responsiveness of copolymers creates a synergistic effect that optimizes CDI performance, especially for selective ion removal or operation under extreme pH conditions.

Recent research has demonstrated that incorporating pH-responsive polymers strengthens electrostatic interactions between the electrode and target ions, resulting in improved electrosorption capacity. Xiong and collaborators developed a versatile CNT membrane electrode by combining CNTs with the pH-responsive block copolymer poly(2-dimethylaminoethyl methacrylate)-block-polystyrene (PDMAEMA-b-PS)[195]. Fig. 4c shows the fabrication process, which involves blending PDMAEMA-b-PS with CNTs, casting the membrane, and using selective swelling to expose PDMAEMA blocks on the membrane surface. During CDI operation, the PDMAEMA blocks, which contain tertiary amine groups ($-N(CH_3)_2$), become protonated in acidic environments with pH < 6. This protonation generates positively charged $-N^+(CH_3)_2$ sites that strongly attract anions such as Cl^- and $H_2PO_4^-$.

Experimental results highlighted the importance of solution pH in determining CDI performance. At the optimal pH of 5 for anion removal, the PDMAEMA-b-PS/CNT electrode reached maximum electrosorption capacities of approximately 15 mg g^{-1} for NaCl and about 38.7 mg g^{-1} for NaH_2PO_4 when tested in 100 mg L^{-1} NaCl and 50 mg L^{-1} NaH_2PO_4 solutions, respectively. The electrode also showed a $H_2PO_4^-/Cl^-$ selectivity ratio between 8 and 10. Importantly, the electrode demonstrated improved mechanical and chemical stability. After 10 charge-discharge cycles at 1.2 V, performance degradation remained < 5%, with no observed anode oxidation. The swollen layer of the copolymer also created a steric barrier that eliminated the typical co-ion repulsion effect, preventing the 15%-20% capacity loss commonly seen in conventional CDI electrodes while improving energy efficiency by 25% to 30%[195].

3.5 CNT-metal compound composite electrodes

Metal compounds, such as Titanium dioxide (TiO_2), Manganese dioxide (MnO_2) and Molybdenum disulfide (MoS_2), have gained immense attention in the field of CDI due to their inherent pseudocapacitive nature and high ion electrosorption capacities[196–197]. The metal oxides can undergo fast and reversible Faradaic processes, allowing for better charge storage than the electrical double-layer capacitance mechanism prevalent in carbonaceous materials.

Thus, their intercalation with CNTs actually improves the total charge storage ability, thus leading to improved electrochemical performance and improved desalination efficiency[198].

The incorporation of metal compounds into CNT composites enhances electrode performance through two primary mechanisms. First, these additives increase the natural capacitance and wettability of the electrodes, facilitating greater electrolyte penetration and enhanced ion migration. Metal oxides further contribute by providing active sites for ion electrosorption, enabling more selective and efficient ion removal[199]. This synergistic combination is particularly effective as CNTs form conductive networks that compensate for the poor inherent conductivity of many metal oxides, promoting rapid electron transfer and optimal charge redistribution.

Second, the integration of CNTs with metal compounds significantly improves the structural stability and durability of electrode materials[200]. Unlike metal oxides, which typically suffer from volume expansion and structural degradation during repeated charge-discharge cycles, CNTs provide essential mechanical support and elasticity. These properties effectively mitigate deformation effects and substantially extend electrode lifespan. The resulting structural enhancement also enables superior regeneration capability, allowing numerous electrosorption-desorption cycles to occur without significant performance degradation.

3.5.1 CNT-based titanium (Ti) compound electrodes

TiO_2 has been extensively investigated as a CDI electrode material due to its attractive combination of high chemical stability across a wide pH range (3-11), low cost, and inherent pseudocapacitive behavior[201–202]. Nevertheless, pure TiO_2 suffers from intrinsic drawbacks, including low electrical conductivity and a limited specific surface area, which restrict charge transfer and ion electrosorption. These disadvantages can be overcome by combining TiO_2 with CNTs. CNTs possess high electrical conductivity and a large specific surface area. When composited with TiO_2, they form conductive networks that facilitate electron transport and create tubular channels for ion diffusion, thereby enhancing CDI performance.

Although CNTs exhibit excellent conductivity, their inherent hydrophobicity and lack of pseudocapacitance limit their ion removal efficiency. To address these issues, atomic layer deposition (ALD) has been employed to coat TiO_2 nanoparticles onto CNT membranes, resulting in improved electrosorption capacity and enhanced hydrophilicity[201]. ALD allows precise control over TiO_2 film thickness and uniformity, thereby strengthening the interfacial interaction between CNTs and TiO_2. This modification increases the available surface area for ion adsorption and reduces the water contact angle of CNT membranes to around 60°–70°, which promotes electrolyte infiltration and ion conductivity. Furthermore, TiO_2 introduces pseudocapacitive charge storage through the reversible Ti^{3+}/Ti^{4+} redox couple, which further improves the electrochemical performance of the composite electrode.

Feng et al. prepared TiO_2-decorated CNT membranes by ALD for CDI applications[202]. As illustrated in Fig. 5a, the process included pretreatment of the CNT membrane by plasma cleaning to improve surface adhesion, alternating pulses of titanium tetraisopropoxide and water as precursors, and purging to remove unreacted species. After 20 deposition cycles, a uniform TiO_2 film of about 20 nm thickness was obtained. The resulting CNT-TiO_2 membranes showed significantly improved CDI performance. In a 50 mg L^{-1} Cr(VI) solution at 1.2 V, the removal efficiencies of total Cr and Cr(VI) reached 92.1% and 93.3%, respectively, which was 30%−40% higher than that of pristine CNT membranes. Cycling tests demonstrated good durability, with the Cr(VI) removal efficiency maintained at approximately 93% after four cycles. These results confirm ALD as an effective method for fabricating high-performance CDI electrodes and highlight its potential in electrochemical water purification[202].

The choice of preparation method has a direct impact on the structure and electrochemical properties of CNT/TiO_2 electrodes and, consequently, on

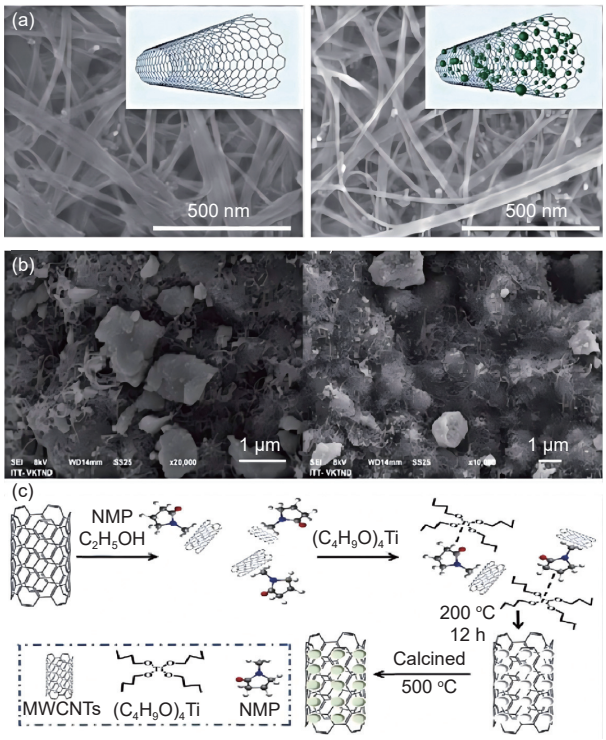

Fig. 5 (a) SEM images of CNT-based electrodes and CNT/TiO_2 electrodes. Copyright 2021, Elsevier. (b) SEM images of CNT/TiO_2 electrode. Copyright 2023, Wiley. (c) Synthetic schemes of TiO_2/CNT composites. Copyright 2021, IWA Publishing

their ion removal performance. In addition to ALD, the sol-gel method represents another reliable and versatile fabrication route. This solution-based approach enables the deposition of porous and compositionally tunable TiO_2 coatings on CNTs. Titanium alkoxide precursors, such as tetrabutyl titanate, undergo hydrolysis and condensation to form a gel, which is subsequently heat-treated at 400–600 °C to yield crystalline TiO_2. The sol-gel method is scalable, compatible with carbon substrates, and allows tuning of pore structure, which is crucial for enhancing electrosorption capacity and charge storage performance[203].

Nguyen et al. synthesized CNT/TiO_2 composites by the sol-gel method and systematically evaluated their CDI performance. As shown in Fig. 5b, the fabrication process involved the hydrolysis of titanium alkoxides in ethanol, dispersion of CNTs into the resulting sol, film casting, and subsequent heat treatment at 500 °C to generate porous TiO_2. The obtained composite electrode exhibited a mesopore volume of 0.3–0.5 cm^3 g^{-1}, which reduced ion diffusion resistance by 40%–50% compared with pure TiO_2. In CDI experiments with a 200 mg L^{-1} NaCl solution at 1.4 V, the electrode achieved a salt electrosorption capacity of 17.5 mg g^{-1} and a charge efficiency of 90%. In addition, the capacitance remained unchanged after 3000 cycles, demonstrating excellent long-term stability[203].

Another frequently used technique for fabricating CNT/TiO_2 composites is the solvothermal process. In this method, titanium precursors such as titanium tetrachloride are dissolved in a solvent, for example N-methylpyrrolidone (NMP), and subjected to a controlled reaction in a sealed autoclave at 180–220 °C[204]. This process enables uniform deposition of TiO_2 nanoparticles with sizes of 10–15 nm on CNTs, preventing agglomeration while allowing control over particle size, crystallinity, and morphology, which are critical for electrochemical performance.

Ma et al. reported a solvothermal strategy for preparing CNT/TiO_2 composites. As illustrated in Fig. 5c, the process involved mixing titanium precursors with CNTs in NMP, reacting at 200 °C for 12 h in an autoclave, followed by washing to remove impurities. The resulting composite displayed outstanding electrochemical characteristics, including a specific capacitance of 87.6 F g^{-1} and a maximum electrosorption capacity of 6.5 mg g^{-1} for chloride ions in a 100 mg L^{-1} NaCl solution at 1.2 V, which was 2 to 3 times higher than that of pure TiO_2. Furthermore, the electrode maintained stable dechlorination efficiency over 5 consecutive cycles without noticeable degradation, indicating good long-term applicability[204].

Overall, each synthesis method provides distinct advantages depending on the CDI application. ALD offers atomic-level precision and is particularly effective for heavy metal removal. The sol-gel method supports large-scale fabrication and is suitable for cost-effective brackish water treatment. The solvothermal process enables uniform nanoparticle distribution and is advantageous for selective anion removal. Consideration of these trade-offs is essential for selecting the most appropriate synthesis method for specific elec-

trochemical water treatment scenarios[201–204].

3.5.2 CNT-based molybdenum (Mo) compound electrodes

CNT-Mo compound composites, particularly CNT/MoS_2, have shown promising performance in CDI due to the complementary properties of the 2 components[205]. MoS_2 alone is attractive for CDI because of its pseudocapacitive nature, but it suffers from low electrical conductivity (10^{-6}–10^{-3} S cm^{-1}) and a tendency for severe layer restacking (interlayer distance around 0.62 nm), which hinders charge transport and restricts ion access[150]. Incorporating CNTs can effectively overcome these drawbacks. CNTs, with high conductivity (10^4–10^6 S m^{-1}), provide a 3D conductive framework that accelerates electron transfer, while their tubular structure prevents MoS_2 nanosheets from restacking by expanding the interlayer spacing to 0.8-1.0 nm. This structural design creates continuous ion transport channels and exposes more active sites, combining the electric double-layer capacitance of CNTs with the Faradaic activity of MoS_2, thereby enhancing both electrosorption capacity and cycling stability[206].

Cai et al. prepared a high-performance electrode by assembling few-layer MoS_2 nanosheets with a CNT network through a hydrothermal method. As shown in Fig. 6a, the process involved synthesizing MoS_2 nanosheets with lateral sizes of 50-100 nm, dispersing CNTs into the suspension, and constructing a three-dimensional interconnected structure. The composite displayed 2 key advantages. First, the expanded MoS_2 interlayer spacing of about 0.9 nm created numerous Faradaic-active sites for reversible Mo^{4+}/Mo^{6+} redox reactions, which accounted for 60%–70% of the total capacitance. Second, the CNT framework lowered the water contact angle from more than 90° for pure MoS_2 to about 65°–70°, improved electron transfer, and reduced charge transfer resistance by 40%–50%. In CDI experiments with a 300 mg L^{-1} NaCl solution at 1.2 V, the electrode achieved a salt electrosorption capacity of 25.35 mg g^{-1}, which was 3 to 4 times higher than that of pure MoS_2 (6–8 mg g^{-1}) and about 1.5 times higher than pure CNTs (16–18 mg g^{-1}). Long-term stability was also confirmed, with the electrode retaining 98.8% of its initial capacity after 30 electrosorption/desorption cycles[206].

In addition to serving as standalone CDI electrodes, CNT/MoS_2 composites can also be used to modify other 2D materials such as MXenes, thereby addressing their inherent shortcomings while maintaining synergistic advantages. MXenes are attractive for electrochemical applications because of their high specific capacitance (300–400 F g^{-1}), rapid ion intercalation kinetics, and good hydrophilicity (water contact angle around 40°–50°). However, their practical application is limited by 2 major problems. First, MXenes are prone to oxidation. For instance, $Ti_3C_2T_x$ can oxidize in air within 7–10 days, forming TiO_2 and losing 30%–40% of its capacitance. Second, their strong interlayer restacking reduces ion transport channels and lowers electrosorption efficiency[207].

To address these issues, Zargar et al. proposed a one-step hydrothermal method to prepare $Ti_3C_2T_x$ MXene/CNT-MoS_2 heterostructures. As illustrated in Fig. 6b, the procedure included exfoliation of $Ti_3C_2T_x$ into few-layer sheets, addition of ammonium molybdate and thiourea as MoS_2 precursors, incorporation of CNTs, and subsequent hydrothermal treatment at 200 °C to build a 3D framework. In the resulting heterostructure, MoS_2 nanosheets acted as spacers to expand the MXene interlayer distance from 0.98 nm to 1.2–1.5 nm, thus alleviating restacking and providing wider ion diffusion channels. CNTs formed continuous conductive bridges between MXene and MoS_2, which reduced charge transfer resistance by 50%–60%. At the same time, the CNT/MoS_2 coating protected MXene against oxygen and water, extending its shelf life to more than 30 days and limiting oxidation-induced capacitance loss to less than 10%. In CDI experiments with a 500 mg L^{-1} NaCl solution at 1.2 V, the heterostructure exhibited a salt electrosorption capacity of 25.82 mg g^{-1}, about 40%–50% higher than that of pure $Ti_3C_2T_x$ MXene (17–18 mg g^{-1}). After ten charge-discharge cycles, it retained 98.1% of its initial desalination capacity, indicating excellent

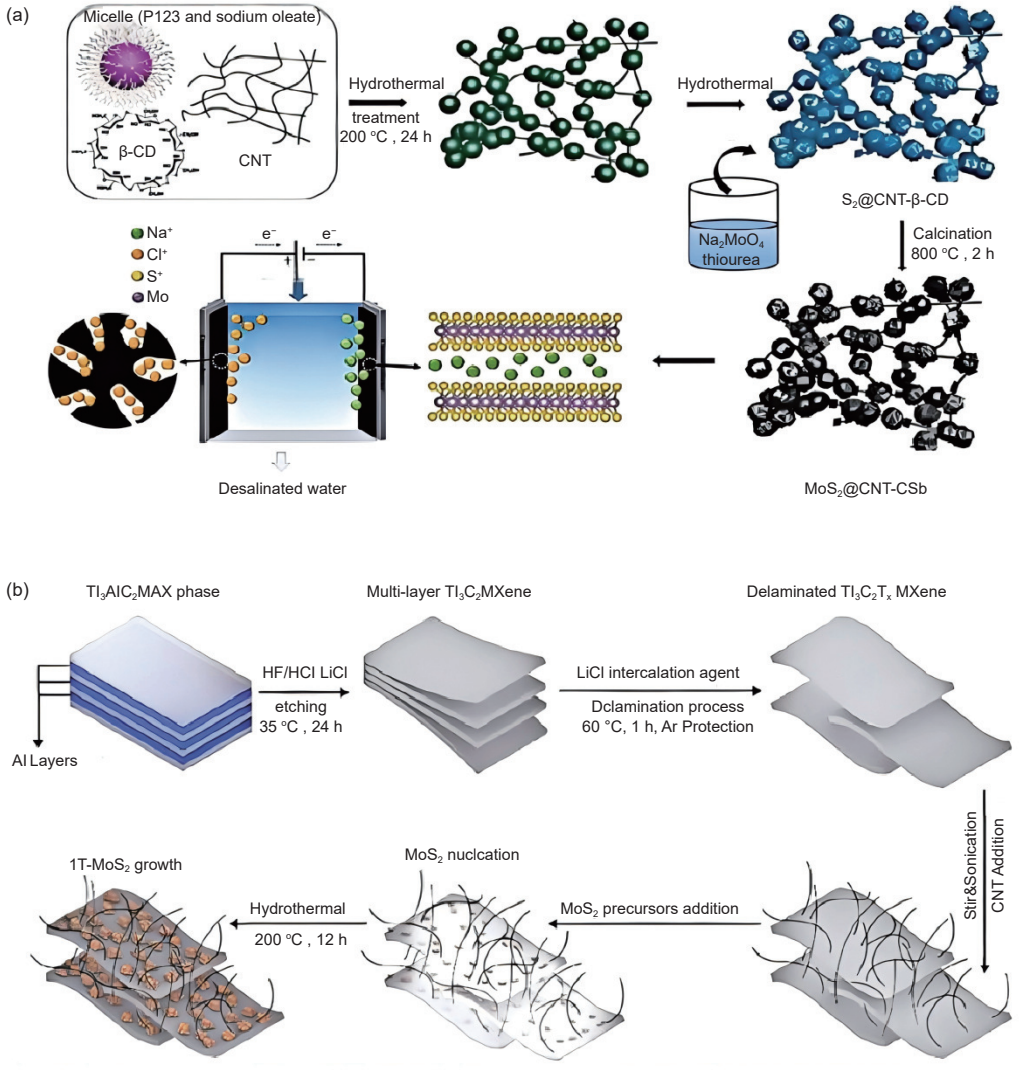

Fig. 6 (a) The synthesis process of the MoS_2/CNT sample. Copyright 2021, Elsevier. (b) Schematic illustration of MoS_2/CNT composite. Copyright 2024, Elsevier

cycling stability[208].

3.5.3 CNT-based Mn compound electrodes

Mn-based compounds such as MnO_2 and Mn_3O_4 have been extensively studied as electrode materials for CDI because of their high theoretical capacitance (~ 1370 F g^{-1} for MnO_2), multiple redox states (Mn^{2+}/Mn^{3+}/Mn^{4+}) that enable reversible Faradaic reactions and low cost[209]. Among them, MnO_2 is the most widely investigated, owing to its excellent electrochemical performance, natural abundance, and environmental friendliness[210]. The crystal structure of MnO_2 strongly affects its properties. In particular, MnO_2, with a layered structure, provides more accessible ion intercalation channels and a higher density of active sites compared with other polymorphs, making it especially suitable for CDI.

Despite these advantages, MnO_2 alone faces significant challenges. Its intrinsic conductivity is very low (10^{-5}–10^{-3} S cm^{-1}), which limits charge transport, and it undergoes considerable volume expansion (20%–30%) during repeated redox cycling. This often leads to structural degradation and more than 50% loss of capacitance after about 100 cycles[211]. To mitigate these problems, MnO_2 is frequently combined with CNTs. CNTs provide continuous conductive pathways, which reduce charge transfer resistance by 60%–70%. Their high mechanical strength also helps to restrain MnO_2 volume expansion to below 5%. As a result, CNT/MnO_2 composites exhibit higher electrosorption capacity, improved charge storage, and en-

hanced cycling durability[212–213].

Material design and interfacial engineering are crucial for maximizing the synergy between CNTs and MnO_2. By carefully controlling the interaction between the two components, it is possible to optimize pore structure, strengthen interfacial bonding, and improve electron transport[214]. Self-assembly approaches have proven especially effective in constructing CNT/MnO_2 composites with high conductivity and porous architectures that promote ion diffusion and charge storage.

Wang et al. reported a self-assembled CNT/MnO_2 composite with excellent CDI performance. As illustrated in Fig. 7a, bulk MnO_2 was exfoliated into nanosheets with lateral sizes of 200–300 nm, which were then dispersed with CNTs to form an expanded lamellar structure. This process increased the MnO_2 interlayer spacing from 0.44 nm to about 0.8–1.0 nm, thereby creating efficient ion transport channels. When tested in a 500 mg L^{-1} NaCl

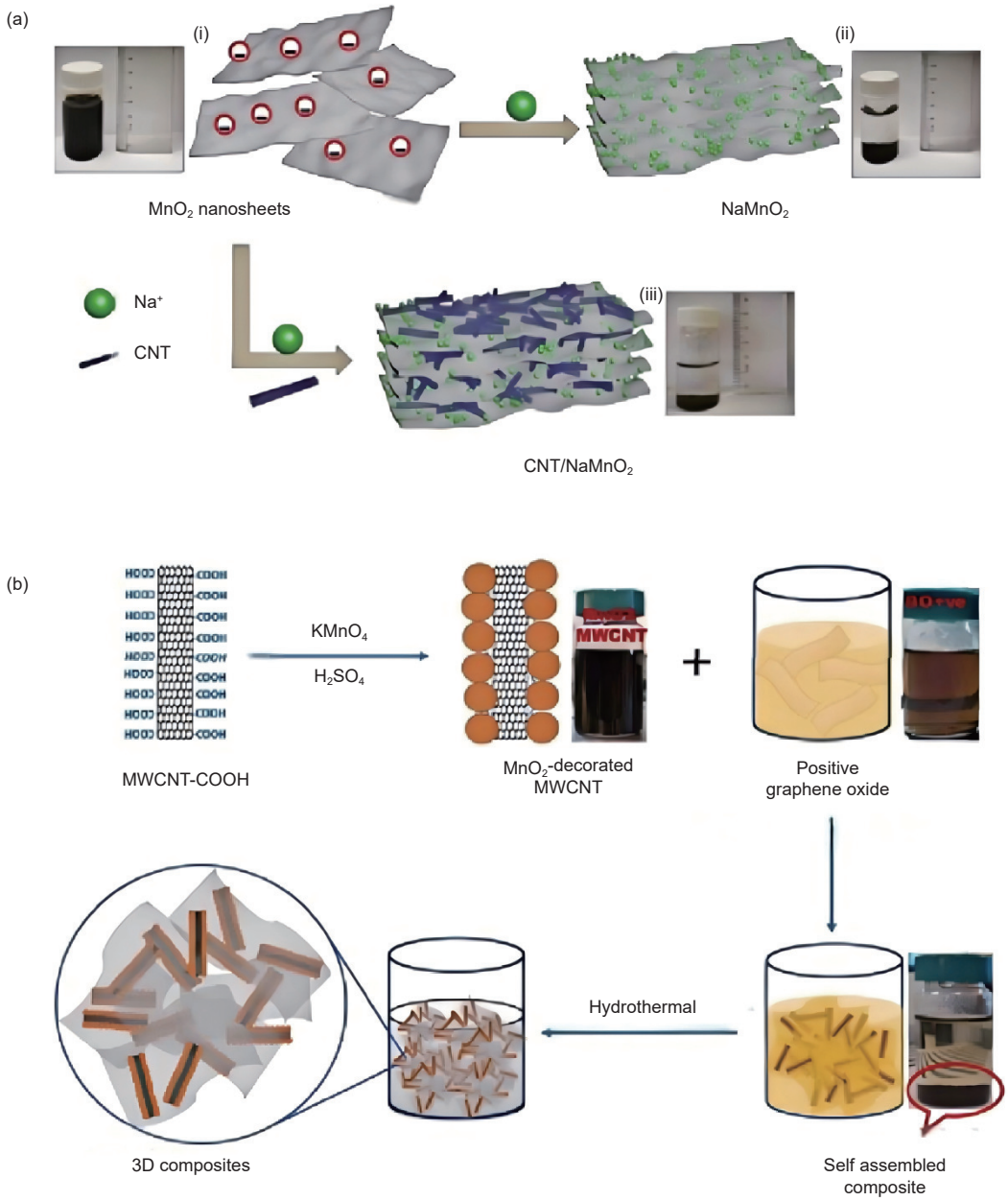

Fig. 7 (a) Schematic illustration for the synthesis of CNT/$NaMnO_2$. Copyright 2019, The Royal Society of Chemistry. (b) Schematic illustration of the method followed in synthesizing the 3D nanocomposites. Copyright 2022, Elsevier

solution at 1.2 V, the composite achieved an ion removal capacity of 42.6 mg g^{-1}, which was 4 to 5 times greater than pure MnO_2 (8–10 mg g^{-1}) and twice that of CNTs alone (20–22 mg g^{-1}). Moreover, the electrode maintained 93% of its initial capacity after 100 cycles, demonstrating outstanding durability. This was attributed to the mechanical support of CNTs, which prevented nanosheet peeling, and to the expanded interlayer spacing, which reduced stress during ion intercalation[215].

Wadi et al. proposed another method for preparing CNT/MnO_2 composites by combining self-assembly with electrostatic co-precipitation. The process (Fig. 7b), included surface modification of CNTs to introduce carboxyl groups, electrostatic adsorption of Mn^{2+} ions on the CNTs, oxidation to form MnO_2, and subsequent hydrothermal treatment at 180 °C for 12 h to strengthen interfacial bonding. This approach yielded a stable 3D porous network with hierarchical pores ranging from 10 to 50 nm and a specific surface area of 250–300 m^2 g^{-1}, about 3 to 4 times higher than that of pure MnO_2. In CDI experiments with a 600 mg L^{-1} NaCl solution at 1.2 V, the composite demonstrated a high electrosorption capacity of 65.1 mg g^{-1}, highlighting its great potential for practical water treatment applications[216].

3.6 CNT-porous carbon composite electrodes

Porous carbon materials such as activated carbon (AC), biochar (BC), and carbon microspheres (CMs) have been widely used in CDI electrodes thanks to their high specific surface area, well developed pore structure and low cost. However, their performance is often limited by poor electrical conductivity, structural instability during cycling, and a tendency for pores to agglomerate. These drawbacks restrict further improvements in CDI efficiency and durability. A promising approach to address these challenges involves incorporating carbon nanotubes into porous carbon matrices.

3.6.1 CNT-based AC electrodes

AC is widely used as an electrode material in CDI and FCDI systems due to its high specific surface area, well-developed pore structure, and low cost, making it highly suitable for real-world applications. These characteristics allow AC to provide abundant active sites for ion electrosorption through electric double-layer capacitance, making it effective for desalination and heavy metal removal[217]. However, unmodified AC has several limitations: its poor electrical conductivity leads to high charge transfer resistance, and when formulated into slurries, the particles often lack continuous contact, further reducing charge transport efficiency. Previously, researchers attempted to address the conductivity issue by using higher AC loadings. However, this increased the viscosity of the slurry, often resulting in clogging issues and higher energy consumption[218]. A more effective solution is to composite AC with CNTs. CNTs exhibit excellent electrical conductivity and a tubular structure that facilitates the formation of a continuous conductive network within the AC electrode. This enhances electron transfer, reduces electrical resistance, and prevents particle agglomeration. As a result, the integration of CNTs significantly improves desalination performance, ion selectivity, and long-term stability in FCDI systems through synergistic effects[219].

Most AC electrodes for CDI are fabricated by the slurry coating method. For a long time, these electrodes have faced 2 key issues. One is that their electron transfer rates fail to meet practical needs, and the other is that they peel off from the substrate during extended operation[220–221]. To solve these problems, Xie et al. proposed a modification strategy for AC electrodes[222]. This approach includes 2 core steps. The first step is to carbonize the binders which typically have poor conductivity to enhance the overall electrical continuity of the electrode. The second step is to use a one-step vacuum chemical vapor deposition (CVD) process to graft CNTs in-situ across the entire AC electrode, and the specific preparation process is illustrated in Fig. 8a. The in-situ grafted CNTs distribute more uniformly within the AC electrode structure. They do not simply mix with AC particles but act as "conductive bridges" to connect individual AC particles tightly, forming a robust and highly conductive carbon framework. This structural improvement

directly leads to better performance. Compared with traditional unmodified AC electrodes, the CNT/grafted AC electrode achieves a notable salt adsorption capacity of 15.6 mg g^{-1}. More importantly, it shows strong long-term reliability. Even after 60 consecutive charge-discharge cycles, the CNT/AC electrode retains its adsorption capacity stably without obvious performance degradation. This confirms the electrode's excellent cycling stability and reproducibility, making it more suitable for practical CDI applications.

In addition to more complex fabrication methods such as chemical vapor deposition, even electrodes prepared by simple physical blending of CNTs and AC exhibit commendable electrochemical performance. Chand and colleagues fabricated flow electrodes by physically integrating AC with CNTs, and systematically evaluated the system performance under varied operational conditions[223]. The introduction of CNTs into the AC-based flow electrode mitigated inter-tube aggregation, enhanced interparticle contact between AC particles, established a continuous conductive network, and improved the overall electrical conductivity of the slurry electrode, thereby promoting efficient Cr(VI) removal. Results indicated that incorporating only 1.5% of CNTs into the AC matrix under an applied voltage of 0.9 V led to a 3.4-fold increase in current response compared to the pure AC electrode. This synergistic enhancement concomitantly achieved a notable Cr(VI) removal efficiency of 99.5%, underscoring the efficacy of CNT integration in advancing electrode performance for decontamination applications.

3.6.2 CNT-based BC electrodes

BC is a renewable porous carbon material produced from pyrolyzed biomass. It has attracted growing interest as an electrode material in CDI systems, owing to its low cost, naturally hierarchical pore structure, and environmentally friendly nature[224]. These characteristics allow BC to offer abundant active sites for ion electrosorption through EDLC, and also support the value-added reuse of biomass waste. That said, untreated BC electrodes face several challenges that limit their practical performance[225]. Their electrical conductivity is often relatively low, a result of incomplete carbonization and disordered carbon structures, which leads to high charge transfer resistance. When used in slurry configurations, BC particles are prone to agglomeration, which can block pores and hinder efficient ion transport. Furthermore, compared to conventional AC, BC generally exhibits lower specific surface area and inferior structural stability over repeated charging and discharging cycles[226].

To overcome these drawbacks, researchers have turned to compositing BC with CNTs. CNTs contribute excellent electrical conductivity, high mechanical strength, and a unique 1D tubular architecture. Within the BC matrix, they form a continuous conductive network that facilitates electron transport, reduces particle aggregation, and helps optimize the overall pore structure by serving as conductive links between BC particles[227]. This composite strategy preserves the economic and sustainability benefits of BC, while significantly improving its electrochemical properties. As a result, BC/CNT electrodes have emerged as a promising and environmentally sustainable materials platform for high-performance CDI applications[228].

Nguyen and his team fabricated a highly cost-effective electrode with excellent performance by incorporating a small amount of CNTs, only 1%, into coconut shell-derived activated carbon (BC), along with a minor graphene addition to improve electrical conductivity (Fig. 8b)[229]. The prepared BC/CNT composite electrode exhibited outstanding electrochemical properties. When tested in a 200 mg L^{-1} NaCl solution at a scan rate of 5 mV s^{-1}, it demonstrated a specific capacitance of 60 F g^{-1}. Furthermore, under an applied voltage of 1.0 V, the electrode achieved a salt adsorption capacity of 9.58 mg g^{-1} and a salt adsorption rate of 1.51 mg g^{-1} min^{-1}. Notably, due to the synergistic effects between the components, this hybrid additive system at low loading (1%) showed better performance and economic viability compared to using any single additive alone.

3.6.3 CNT-based CMs electrodes

CMs, which are porous carbon materials known for their uniform spherical shape, controllable size,

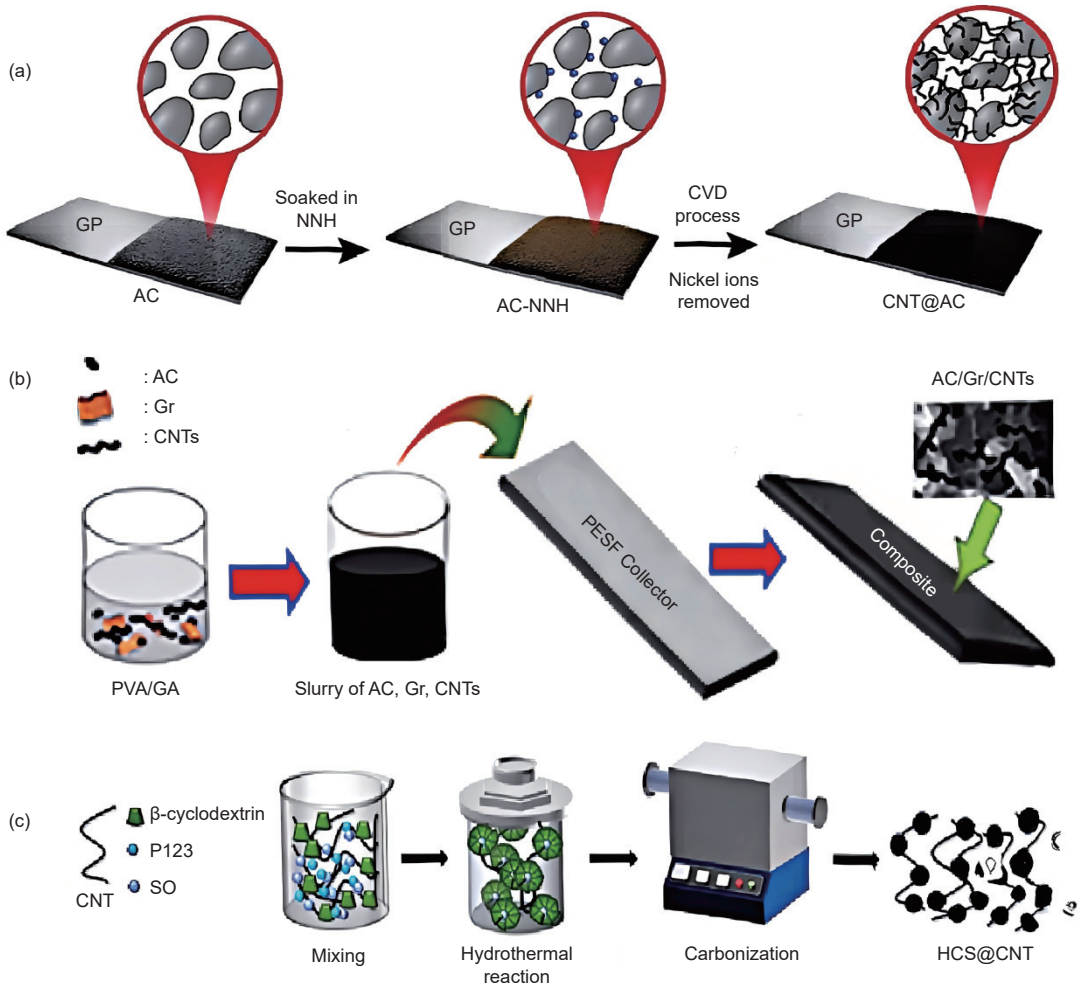

Fig. 8 (a) Schematic illustration for the synthesis of CNT/AC. Copyright 2020, Elsevier; (b) Schematic illustration for the synthesis of CNT/BC. Copyright 2021, Elsevier; (c) Schematic illustration for the synthesis of CNT/CMs. Copyright 2024, Elsevier

and tunable pore structure, have emerged as a promising candidate for electrode materials in CDI[230]. The spherical morphology not only mitigates particle agglomeration but also promotes efficient ion transport[231]. Meanwhile, the adjustable porous framework facilitates ion electrosorption through EDLC, and their inherent chemical stability aligns well with the operational demands of typical CDI systems[232].

Nevertheless, pristine CMs face several limitations. Their electrical conductivity is generally lower than that of CNTs, resulting in higher charge transfer resistance. The often narrowly distributed pore structure also makes it difficult to simultaneously achieve high ion storage and rapid ion transport, particularly in high-salinity environments[233]. Furthermore, CMs tend to exhibit insufficient mechanical strength for long-term use in flowable electrode systems such as FCDI.

To overcome these challenges, researchers have turned to composite strategies incorporating CNTs. The integration of CNTs helps establish a continuous conductive network that significantly enhances electron transfer throughout the electrode. CNTs also serve as structural bridges that improve the mechanical integrity of CMs-based electrodes. In addition, they introduce secondary mesoporous pathways that optimize pore hierarchy for improved ion accessibility. By combining the strengths of CMs and CNTs, this composite approach mitigates the inherent drawbacks of pure CMs, offering a competitive and durable electrode material for high-performance CDI applications[234].

Currently, the performance of CDI is constrained by several technical challenges, including discontinuous conductive networks, inadequate dispersion of suspended carbon particles, and obstructed electron and ion transport pathways. To address these limitations, Cai and colleagues developed a flexible and continuous 3D conductive network, designated CMs/CNTs, by integrating CMs with CNTs using as a flow electrode in CDI systems (Fig. 8c)[235]. The incorporation of HCS significantly improved the fluidity and collision efficiency of the flow electrode slurry. Meanwhile, CNTs facilitated the formation of interconnected pathways that enable smooth ion transport and rapid electron transfer. Furthermore, the spherical CMs structures served as fluid nodes that effectively mitigated the agglomeration tendency of CNTs. As a result, the deliberately engineered CMs/CNT flow electrode demonstrated favorable rheological properties, along with high hydrophilicity, elevated specific capacitance, and low ion diffusion resistance. When treating a high-concentration NaCl solution (10 g L^{-1}), the electrode achieved a salt removal capacity of 197 mg g^{-1}. Notably, it maintained consistent stability and operational continuity throughout a 10-h continuous desalination test, highlighting its strong potential for high-salinity brine treatment applications.

3.7 CNT-metal-organic frameworks composite electrodes

Metal-organic frameworks (MOFs) are promising CDI electrode materials due to their exceptionally high surface area, tunable porosity, and versatile chemical functionality[236]. These properties allow them to provide numerous active sites for ion adsorption and support selective ion removal. However, the practical application of MOFs in CDI is often limited by their inherently low electrical conductivity, which restricts efficient charge transfer during the electrosorption process[237].

To overcome this challenge, researchers have integrated CNTs into MOF-based electrodes. CNTs contribute high electrical conductivity, mechanical strength, and a unique one-dimensional structure that makes them an excellent complementary material[238]. In such composites, CNTs enhance electrical conduction throughout the electrode and also provide mechanical support that helps prevent MOF particles from agglomerating or degrading over repeated charging and discharging cycles. This improvement significantly boosts the electrode's cycling stability[239].

Moreover, the combination of CNTs and MOFs creates a synergistic effect that improves surface wettability and promotes optimized ion transport pathways. These enhancements lead to greater electrosorption capacity and faster deionization kinetics[240]. As a result, CNT/MOF composites have gained increasing attention as high-performance materials capable of advancing CDI technology[241].

Phuoc et al. developed a ZIF-67 composite using CNTs as a supporting framework, effectively integrating the advantages of MOFs and nanocarbon materials for application in CDI electrodes (Fig. 9a)[242]. Their results demonstrated that incorporating 30% ZIF-67/CNT into the electrode led to an 88% enhancement in salt removal performance compared with pristine AC. Further electrochemical characterization using cyclic voltammetry and electrochemical impedance spectroscopy confirmed that the composite electrode exhibited reduced electrical resistance and increased capacitance. In CDI tests conducted with a 500 mg L^{-1} NaCl solution, the electrode achieved a salt adsorption capacity of 11.32 mg g^{-1}. Moreover, the electrode maintained stable performance over 25 consecutive charge-discharge cycles (1000 min), indicating excellent cycling durability.

Akulwar and colleagues employed a straightforward one-step hydrothermal approach to synthesize Fe-MOF/CNT composites. In this process, multi-walled carbon nanotubes were dispersed in a solution of ferric chloride, formic acid, and dimethylformamide, and the mixture was reacted at 100 °C for 6 h (Fig. 9b)[243]. The resulting composite forms a conductive network that facilitates efficient electron transport and provides ample pathways for ion diffusion. These structural advantages contribute to an outstanding desalination performance, including a remarkable salt adsorption capacity of 80.575 mg g^{-1}

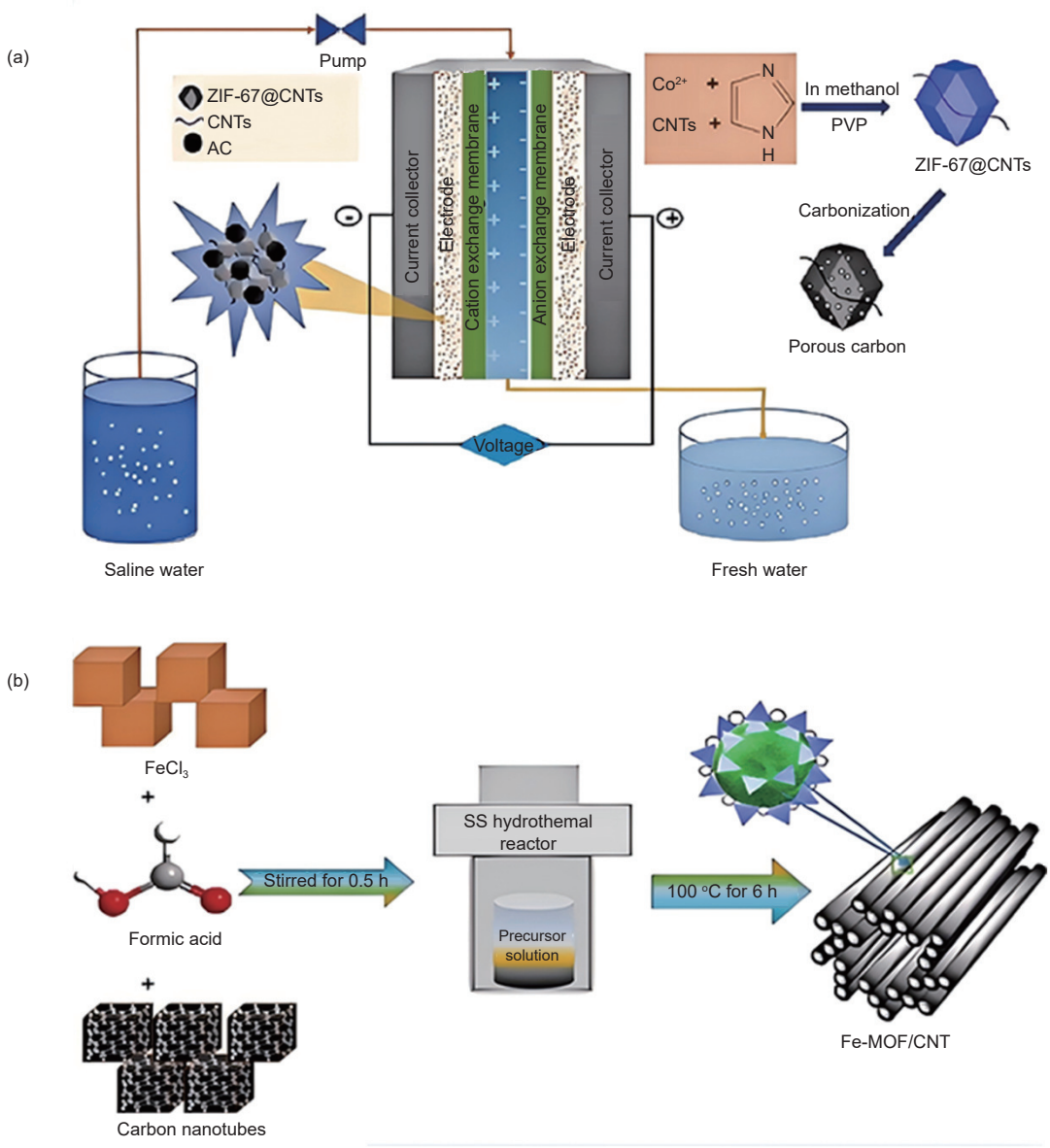

Fig. 9 (a) Schematic illustration for the synthesis of ZIF-67/CNT. Copyright 2020, MDPI. (b) Schematic illustration for the synthesis of Fe-MOF/CNT. Copyright 2024, Springer Nature

when treating a 1000 mg L^{-1} NaCl solution at 1.6 V. Moreover, the electrode demonstrates excellent cycling stability, retaining its performance over 100 consecutive cycles without significant decay. A key strength of this synthesis route is its simplicity, which streamlines production and enhances process efficiency. Unlike conventional methods that often involve multiple steps, high-temperature treatments, or intricate post-processing, this approach reduces both energy consumption and preparation time while also curtailing potential pollution. The use of inexpensive and readily available precursors, such as iron salts and carbon nanotubes, further helps keep material costs low. This efficient and user-friendly synthesis method shows strong potential for scaling up electrode production and advancing practical applications in capacitive deionization.

The diverse strategies for designing and synthesizing CNT-based electrode materials, as discussed in Sections 3.1 to 3.7, are comprehensively summarized in Fig. 10 and Table 1. This schematic illustrates the architectural designs, composite components, and synergistic advantages that contribute to enhanced CDI performance, while the table presents a detailed quant-

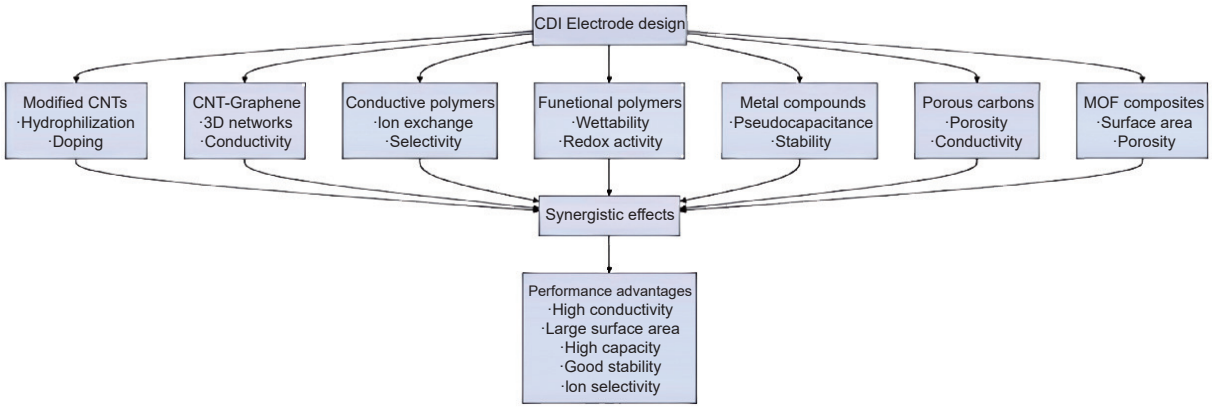

Fig. 10 Design strategies and synergistic advantages of CNT-based CDI electrodes

Table 1 Various carbon materials and their capacitive deionization performance

electrode	Voltage /V	Solution /(NaCl, mg L^{-1})	Specific capacitance /(F g^{-1})	Electrosorption capacity /(mg g^{-1})	CDI Decay rate (%)/cycles	Refs.
CNTs	1	1000	160.4 at 0.5 A g^{-1}	139	3/5	[141]
CNTs	1.2	584	158.6 at 0.5 A g^{-1}	17.2	0/20	[146]
CNTs	1.2	500	23.8 at 50 mV s^{-1}	58.2	0/10	[149]
CNT/graphene	1.2	500	243.2 at 0.5 A g^{-1}	16.5	0/15	[152]
CNT/graphene	2.0	300	36.4 at 1 mV s^{-1}	48.7	-	[158]
CNT/graphene	1.2	500	-	13.6	0/20	[162]
CNT/PPy	1.2	500	96.8 at 5 mV s^{-1}	35.5	8.9/20	[174]
CNT/SBE-β-CD	1.2	500	60.9 at 5 mV s^{-1}	6.4	4.4/50	[185]
CNT/PEDOT:PSS	1.2	60000	-	955.0	-	[189]
CNT/PDMAEMA-b-PS	1.2	100	-	6.4	0/10	[195]
CNT/TiO_2	1.4	200	178 at 1 A g^{-1}	17.5	-	[203]
CNT/TiO_2	1.2	200	87.6 at 1 mV s^{-1}	6.5	0/5	[204]
CNT/MoS_2	1.2	500	140.0 at 0.5 A g^{-1}	25.4	1.2/5	[206]
CNT/MoS_2	1.2	500	140.0 at 5 mV s^{-1}	25.8	1.9/5	[208]
CNT/MnO_2	1.2	500	189.5 at 2 mV s^{-1}	42.6	1.9/5	[215]
CNT/MnO_2	1.2	600	19.0 at 1 mV s^{-1}	65.1	-	[216]
CNT/AC	1.5	1000	84.0 at 1 mV s^{-1}	15.6	0/60	[222]
CNT/BC	1	200	60.0 at 5 mV s^{-1}	9.6	-	[229]
CNT/CM	1.2	10000	125.0 at 5 mV s^{-1}	197	-	[235]
CNT/MOF	1.2	500	96.6 at 1 mV s^{-1}	11.3	0/25	[242]
CNT/MOF	1.6	1000	114.5 at 10 mV s^{-1}	80.6	0/100	[243]

itative comparison of the key electrochemical and desalination performance metrics of various CNT-based electrodes under different test conditions.

4 Conclusions and prospects

This comprehensive review systematically examines the scientific and technological advances in CNT-based electrode materials for CDI. Through a critical analysis of material architectures, synthesis methodologies, and performance characteristics, it is demonstrated that CNTs and their composite derivatives represent a significant advancement in electrochemical desalination technologies. The fundamental attributes of CNTs, including their high aspect ratio, exceptional mechanical strength, and superior electrical conductivity, constitute the basis for their outstanding electrochemical performance. When combined with versatile surface modification enabled by chemical functionalization, these intrinsic properties have facilitated the development of advanced electrode systems that substantially outperform conventional carbon-based materials.

The strategic integration of CNTs with complementary materials such as graphene, conductive poly-

mers, metal oxides, porous carbons, and metal organic frameworks has yielded composite electrodes exhibiting synergistic effects that enhance multiple CDI performance parameters. These advanced materials consistently demonstrate salt adsorption capacities ranging from 25 to 65 mg g^{-1}, with optimized configurations achieving even higher values under specific operational conditions. The composite electrodes typically exhibit specific capacitance values exceeding 200 F g^{-1}, while maintaining exceptional cycling stability. Most systems preserve over 90% of their initial capacity after 100 charge-discharge cycles. These performance enhancements primarily originate from rational material design that effectively combines the superior charge transport properties of CNTs with additional functionalities provided by secondary components, including pseudocapacitive contributions, improved hydrophilicity, and optimized pore structure engineering.

Despite these notable achievements, several substantial challenges impede the practical implementation of CNT based CDI systems and require focused research attention. Electrode fouling caused by organic contaminants and mineral scaling from multivalent ions presents significant limitations to long term operational stability, typically resulting in performance degradation of 15% to 20% during extended operation. The chemical stability of CNT based electrodes under extreme pH conditions or elevated operating voltages remains concerning, particularly for functionalized variants where surface modifications may introduce vulnerabilities to electrochemical degradation. Economic considerations constitute another major barrier, as high purity CNTs, especially single walled varieties or those with specific functionalization, rendering large scale deployment economically challenging. Furthermore, synthesis protocols for high performance CNT composites often involve complex, energy intensive processes such as chemical vapor deposition, solvothermal treatment, and atomic layer deposition, creating significant obstacles for mass production and consistent quality control. The scalability of these manufacturing methods while maintaining precise control over critical parameters including CNT alignment, distribution within composites, and interface engineering represents a formidable challenge that must be resolved to ensure commercial viability.

Future research should prioritize several strategic directions to advance CNT-based CDI technology. The development of cost effective and environmentally sustainable synthesis routes demands immediate attention. Promising approaches include utilizing waste derived precursors, establishing continuous flow synthesis systems, and implementing energy efficient processing methods that could potentially reduce production costs by 30% to 50% while maintaining performance standards. The design of intelligent electrode systems with stimuli responsive characteristics represents another crucial research frontier. Materials capable of adapting their properties in response to variations in water composition, pH levels, or temperature fluctuations would significantly enhance operational flexibility and treatment efficiency. The integration of self cleaning mechanisms through photocatalytic coatings or electrochemically active surfaces could further improve long term stability and reduce maintenance requirements. From a system perspective, the strategic integration of CDI units with renewable energy sources such as solar photovoltaics or wind power, coupled with advanced energy recovery systems during electrode regeneration, could substantially improve overall energy efficiency and economic competitiveness. The establishment of standardized testing protocols and performance evaluation metrics across the research community is equally essential to enable meaningful comparisons between different material systems and accelerate technology transfer. Finally, the implementation of advanced computational methods, including machine learning algorithms for material discovery and multi scale modeling for process optimization, promises to significantly shorten development cycles and enhance system level performance prediction.

Conflicts of interest

The authors declare no conflict of interest.

Acknowledgements

This research was funded by the Joint Funds of the National Natural Science Foundation of China (U1706225), and the Fundamental Research Funds for the Central Universities (201562026, 201762029).

References

[1] Amin M. Incorporation of aluminosilicate into ZIF-activated carbon membrane for H_2/CO_2 and CH_4/CO_2 separation[J]. Journal of the Iranian Chemical Society, 2023, 20: 1457-1468.

[2] Zamankhani R, Rouhani M. Computational insight into hydrogen storage capacity of Ca-deposited B16 system[J]. Journal of the Iranian Chemical Society, 2025, 1-11.

[3] Chairam S, Jarujamrus P, Amatatongchai M. Enhanced catalytic activity in hydrogen production from hydrolysis of sodium borohydride using starch hydrogel-CoNi bimetallic alloys[J]. Journal of the Iranian Chemical Society, 2021, 18: 689-699.

[4] Mishra R K. Fresh water availability and its global challenge[J]. British Journal of Multidisciplinary and Advanced Studies, 2023, 4(3): 1-78.

[5] Van Vliet M T, Jones E R, Flörke M, et al. Global water scarcity including surface water quality and expansions of clean water technologies[J]. Environmental Research Letters, 2021, 16(2): 024020.

[6] Baggio G, Qadir M, Smakhtin V. Freshwater availability status across countries for human and ecosystem needs[J]. Science of the Total Environment, 2021, 792: 148230.

[7] Panagopoulos A. Energetic, economic and environmental assessment of zero liquid discharge (ZLD) brackish water and seawater desalination systems[J]. Energy Conversion and Management, 2021, 235: 113957.

[8] Jarin M, Dou Z, Gao H, et al. Salinity exchange between seawater/brackish water and domestic wastewater through electrodialysis for potable water[J]. Frontiers of Environmental Science & Engineering, 2023, 17(2): 16.

[9] Ramirez-Moreno M, Esteve-Nunez A, Ortiz J M. Desalination of brackish water using a microbial desalination cell: analysis of the electrochemical behaviour[J]. Electrochimica Acta, 2021, 388: 138570.

[10] Honarparvar S, Zhang X, Chen T, et al. Frontiers of membrane desalination processes for brackish water treatment: a review[J]. Membranes, 2021, 11(4): 246.

[11] Stein S, Sivan O, Yechieli Y, et al. An advantage for desalination of coastal saline groundwater over seawater in view of boron removal requirements[J]. Environmental Science: Water Research & Technology, 2021, 7(12): 2241-2254.

[12] Kumar S, Aldaqqa N M, Alhseinat E, et al. Electrode materials for desalination of water via capacitive deionization[J]. Angewandte Chemie, 2023, 135(35): e202302180.

[13] Gamaethiralalage J, Singh K, Sahin S, et al. Recent advances in ion selectivity with capacitive deionization[J]. Energy & Environmental Science, 2021, 14(3): 1095-1120.

[14] Yang F, He Y, Rosentsvit L, et al. Flow-electrode capacitive deionization: a review and new perspectives[J]. Water Research, 2021, 200: 117222.

[15] Zhang C, Ma J, Wu L, et al. Flow electrode capacitive deionization (FCDI): recent developments, environmental applications, and future perspectives[J]. Environmental Science & Technology, 2021, 55(8): 4243-4267.

[16] Wang H, Liu Y, Li Y, et al. Tactics for boosting the desalination stability of capacitive deionization[J]. Chemical Engineering Journal, 2024, 153808.

[17] Shocron A N, Roth R S, Guyes E N, et al. Comparison of ion selectivity in electrodialysis and capacitive deionization[J]. Environmental Science & Technology Letters, 2022, 9(11): 889-899.

[18] Wang H, Xu X, Gao X, et al. Design of three-dimensional faradic electrode materials for high-performance capacitive deionization[J]. Coordination Chemistry Reviews, 2024, 510: 215835.

[19] Zhang B, Boretti A, Castelletto S. MXene pseudocapacitive electrode material for capacitive deionization[J]. Chemical Engineering Journal, 2022, 435: 134959.

[20] Ma J, Zhou R, Yu F. Hotspots and future trends of capacitive deionization technology: a bibliometric review[J]. Desalination, 2024, 571: 117107.

[21] Ma J, Zhai C, Yu F. Review of flow electrode capacitive deionization technology: Research progress and future challenges[J]. Desalination, 2023, 564: 116701.

[22] Tauk M, Bechelany M, Sistat P, et al. Ion-selectivity advancements in capacitive deionization: a comprehensive review[J]. Desalination, 2024, 572: 117146.

[23] Gao M, Chen W. Engineering strategies toward electrodes stabilization in capacitive deionization[J]. Coordination Chemistry Reviews, 2024, 505: 215695.

[24] Sivasubramanian P, Kumar M, Kirankumar V, et al. Capacitive deionization and electrosorption techniques with different electrodes for wastewater treatment applications[J]. Desalination, 2023, 559: 116652.

[25] Datar S D, Mane R, Jha N. Recent progress in materials and architectures for capacitive deionization: A comprehensive review[J]. Water Environment Research, 2022, 94(3): e10696.

[26] AL-Rajabi M M, Abumadi F A, Laoui T, et al. Capacitive deionization for water desalination: cost analysis, recent advances, and process optimization[J]. Journal of Water Process Engineering, 2024, 58: 104816.

[27] Xu X, Eguchi M, Asakura Y, et al. Metal-organic framework derivatives for promoted capacitive deionization of oxygenated saline water[J]. Energy & Environmental Science, 2023, 16(5): 1815-1820.

[28] Yu F, Yang Y, Zhang X, et al. Application of capacitive deionization in drinking water purification[J]. Separation and Purification Technology, 2024, 129285.

[29] Wu Q, Liang D, Lu S, et al. Advances and perspectives in integrated membrane capacitive deionization for water desalination[J]. Desalination, 2022, 542: 116043.

[30] Gao M, Yang Z, Liang W, et al. Recent advanced freestanding pseudocapacitive electrodes for efficient capacitive deionization[J]. Separation and Purification Technology, 2023, 324: 124577.

[31] Ma J, Chen L, Yu F. Environmental applications and perspectives of flow electrode capacitive deionization (FCDI)[J]. Separation and Purification Technology, 2024, 335: 126095.

[32] Liu X, Rehman D, Shu Y, et al. Selective fluoride removal from groundwater using CNT-CeO_2 electrodes in capacitive deionization (CDI)[J]. Chemical Engineering Journal, 2024, 482: 149097.

[33] Rangaraj V M, Yoo J I, Song J K, et al. Three-dimensional (3D) $MnMoO_4$@g-C_3N_4/CNT hybrid composite electrode for hybrid capacitive deionization[J]. Separation and Purification Technology, 2023, 317: 123898.

[34] Zhang H, Wang Q, Zhang J, et al. Development of novel ZnZr-COOH/CNT composite electrode for selectively removing phosphate by capacitive deionization[J]. Chemical Engineering Journal, 2022, 439: 135527.

[35] Zhang S, Ye Z, Ma M, Yin P, Bao Y, Li F. Optimizing the integration of nickel hexacyanoferrate with hollow mesoporous carbon spheres (HMCSs) for highly efficient capacitive deionization[J]. Desalination, 2025, 603: 118679.

[36] Cai Y, Zhang L, Fang R, et al. Maximized ion accessibility in the binder-free layer-by-layer MXene/CNT film prepared by the electrophoretic deposition for rapid hybrid capacitive deionization[J]. Separation and Purification Technology, 2022, 292: 121019.

[37] Guo J, Wang Y, Cai Y, et al. Ni-doping Cu-Prussian blue analogue/carbon nanotubes composite (Ni-CuPBA/CNTs) with 3D electronic channel-rich network structure for capacitive deionization[J]. Desalination, 2022, 528: 115622.

[38] Tang Y, Shi Y, Su Y, Cao S, Hu J, Zhou H, Sun Y, et al. Enhanced capacitive deionization of hollow mesoporous carbon spheres/MOFs derived nanocomposites by interface-coating and space-encapsulating design[J]. Advanced Science, 2024, 11(39): 2403802.

[39] Tabrizi N S, Taleghani M S. Performance of CNT-CNP aerogel as electrode in capacitive deionization system[J]. Carbon Letters, 2023, 33(4): 1253-1263.

[40] Xu L, Ding Z, Chen Y, et al. Carbon nanotube bridged nickel hexacyanoferrate architecture for high-performance hybrid capacitive deionization[J]. Journal of Colloid and Interface Science, 2023, 630: 372-381.

[41] Li Y, Qi J, Li J, Shen J, Liu Y, Sun X, Shen J, Han W, Wang L. Nitrogen-doped hollow mesoporous carbon spheres for efficient water desalination by capacitive deionization[J]. ACS Sustainable Chemistry & Engineering, 2017, 5(8): 6635-6644.

[42] Shahbazi H, Kazemzadeh M, Khachatourian A M, et al. Capacitive deionization and electrochemical performance of a hierarchical porous electrodes enabled by nitrogen and phosphorus doped CNTs and removable NaCl template[J]. Electrochimica Acta, 2024, 507: 145193.

[43] Zhang W, Wei X, Zhang X, et al. Well-dispersed prussian blue analogues connected with carbon nanotubes for efficient capacitive deionization process[J]. Separation and Purification Technology, 2022, 287: 120483.

[44] Peng Z, Zhang D, Shi L, Yan T. High performance ordered mesoporous carbon/carbon nanotube composite electrodes for capacitive deionization[J]. Journal of Materials Chemistry, 2012, 22(14): 6603-6612.

[45] Jimoh O, Jerina Z, Abdul H, et al. A comprehensive review on recently developed carbon based nanocomposites for capacitive deionization: from theory to practice[J]. Separation and Purification Technology, 2018, 207: 291-320.

[46] Gao X, Omosebi A, Landon J, et al. Surface charge enhanced carbon electrodes for stable and efficient capacitive deionization using inverted adsorption-desorption behavior[J]. Energy & Environmental Science, 2015, 8: 897-909.

[47] Hou C, Liang C, Yiacoumi S, et al. Electrosorption capacitance of nanostructured carbon-based materials[J]. Journal of Colloid and Interface Science, 2006, 302(1): 54-61.

[48] Feuerstadt P, Theriault N, Tillotson G. The burden of CDI in the united states: a multifactorial challenge[J]. BMC Infectious Diseases, 2023, 23(1): 132.

[49] Oren Y. Capacitive deionization (CDI) for desalination and water treatment — past, present and future (a review)[J]. Desalination, 2008, 228(1-3): 10-29.

[50] Seo S J, Jeon H, Lee J K, et al. Investigation on removal of hardness ions by capacitive deionization (CDI) for water softening applications[J]. Water Research, 2010, 44(7): 2267-2275.

[51] Cohen I, Avraham E, Soffer A, et al. Water desalination by capacitive deionization - advantages limitations and modification[J]. Ecs Transactions, 2013, 45(17): 43-59.

[52] Jande Y A C, Minhas M B, Kim W S. Ultrapure water from seawater using integrated reverse osmosis-capacitive deionization system[J]. Desalination & Water Treatment, 2015, 53(13): 3482-3490.

[53] Santana D. Design and implementation of an electrical characterization system for membrane capacitive deionization units for the water treatment[J]. Membranes, 2021, 11(12): 947.

[54] Mcsweeney K T, Morris D, Rettle B, et al. Capacitive deionization of NaCl and $NaNO_3$ solutions with carbon aerogel electrodes[J]. Journal of The Electrochemical Society, 1996, 143(1): 159-169.

[55] Chen W, He X, Jiang Z, et al. A capacitive deionization and electro-oxidation hybrid system for simultaneous removal of heavy metals and organics from wastewater[J]. Chemical Engineering Journal, 2023, 451: 139071.

[56] Xu Z, Pang Z, Yan X, et al. Transition metal oxide electrode materials for capacitive deionization[J]. Chemical Engineering Journal, 2024 : 157257.

[57] Jin J, Wang R, Yu K, et al. Imine-based conjugated polymer enables efficient removal of ammonium ion via capacitive deionization[J]. Separation and Purification Technology, 2025, 353: 128290.

[58] Sayed E T, Obaid M, Olabi A, et al. Recent progress on the application of capacitive deionization for wastewater treatment[J]. Journal of Water Process Engineering, 2023, 56: 104379.

[59] Shocron A, Atlas I, Suss M. Predicting ion selectivity in water purification by capacitive deionization: electric double layer models[J]. Current Opinion in Colloid & Interface Science, 2022, 60: 101602.

[60] Xiaobing W, Jinqiu L, Yang L, et al. Numerical analysis of capacitive deionization process using activated carbon electrodes[J]. Water, Air & Soil Pollution, 2021, 232(9): 364.

[61] Lin Y J, Chen C C. Modeling salt adsorption in electrical double layer for capacitive deionization[J]. AIChE Journal, 2023, 69(5): e18018.

[62] McKague M, Fathiannasab H, Agnaou M, et al. Extending pore network models to include electrical double layer effects in micropores for studying capacitive deionization[J]. Desalination, 2022, 535: 115784.

[63] Wu J. Understanding the electric double-layer structure, capacitance, and charging dynamics[J]. Chemical Reviews, 2022, 122(12): 10821-10859.

[64] Härtel A. Structure of electric double layers in capacitive systems and to what extent (classical) density functional theory describes it[J]. Journal of Physics: Condensed Matter, 2017, 29(42): 423002.

[65] Pekala R W, Alviso C T, Kong F M, et al. Aerogels derived from multifunctional organic monomers[J]. Journal of Non-Crystalline Solids, 1992, 145: 90-98.

[66] Zhang D, Shi L, Fang J, et al. Preparation and desalination performance of multiwall carbon nanotubes[J]. Materials Chemistry and Physics, 2006, 97(2-3): 415-419.

[67] Greathouse J A, Feller S E, McQuarrie D A. The modified gouy-chapman theory: comparisons between electrical double layer models of clay swelling[J]. Langmuir, 1994, 10(7): 2125-2130.

[68] Valleau J, Torrie G. The electrical double layer. III. modified gouy−chapman theory with unequal ion sizes[J]. The Journal of Chemical Physics, 1982, 76(9): 4623-4630.

[69] Pilon L, Wang H, d'Entremont A. Recent advances in continuum modeling of interfacial and transport phenomena in electric double layer capacitors[J]. Journal of The Electrochemical Society, 2015, 162(5): A5158-A5178.

[70] Bücker M, Flores Orozco A, Undorf S, et al. On the role of stern - and diffuse - layer polarization mechanisms in porous media[J]. Journal of Geophysical Research: Solid Earth, 2019, 124(6): 5656-5677.

[71] Ma E, Kim J, Chang H, et al. Stern and diffuse layer interactions during ionic strength cycling[J]. The Journal of Physical Chemistry C, 2021, 125(32): 18002-18014.

[72] Rosen L, Baygents J, Saville D. The interpretation of dielectric response measurements on colloidal dispersions using the dynamic Stern layer model[J]. The Journal of Chemical Physics, 1993, 98(5): 4183-4194.

[73] Porada S, Bryjak M, Van Der Wal A, et al. Effect of electrode thickness variation on operation of capacitive deionization[J]. Electrochimica Acta, 2012, 75: 148-156.

[74] Zhao R, Van Soestbergen M, Rijnaarts H, et al. Time-dependent ion selectivity in capacitive charging of porous electrodes[J]. Journal of Colloid and Interface Science, 2012, 384(1): 38-44.

[75] Delgado A, Jiménez M, Iglesias G, et al. Electrical double layers as ion reservoirs: applications to the deionization of solutions[J]. Current Opinion in Colloid & Interface Science, 2019, 44: 72-84.

[76] Porada S, Weinstein L, Dash R, et al. Water desalination using capacitive deionization with microporous carbon electrodes[J]. ACS Applied Materials & Interfaces, 2012, 4(3): 1194-1199.

[77] Stillinger Jr F H, Kirkwood J G. Theory of the diffuse double layer[J]. The Journal of Chemical Physics, 1960, 33(5): 1282-1290.

[78] Henderson D, Boda D. Insights from theory and simulation on the electrical double layer[J]. Physical Chemistry Chemical Physics, 2009, 11(20): 3822-3830.

[79] Schmickler W. Electronic effects in the electric double layer[J]. Chemical Reviews, 1996, 96(8): 3177-3200.

[80] Brown M A, Abbas Z, Kleibert A, et al. Determination of surface potential and electrical double-layer structure at the aqueous electrolyte-nanoparticle interface[J]. Physical Review X, 2016, 6(1): 011007.

[81] Yao S, Zhu Y. Comparison of adsorption properties of different configurations of CDI cells[J]. International Journal of Electrochemical Science, 2021, 16(6): 210627.

[82] Cho Y, Lee K S, Yang S, et al. A novel three-dimensional desalination system utilizing honeycomb-shaped lattice structures for flow-electrode capacitive deionization[J]. Energy & Environmental Science, 2017, 10(8): 1746-1750.

[83] Balaji-Wright A, Wu J, Shocron A N, et al. Understanding degradation of capacitive deionization cells: full-cell simulations with anode corrosion[J]. Desalination, 2024, 587: 117924.

[84] Zhang C, He D, Ma J, et al. Comparison of faradaic reactions in flow-through and flow-by capacitive deionization (CDI) systems[J]. Electrochimica Acta, 2019, 299: 727-735.

[85] Remillard E M, Shocron A N, Rahill J, et al. A direct comparison of flow-by and flow-through capacitive deionization[J]. Desalination, 2018, 444: 169-177.

[86] Feng A, Feng J, Xing W, et al. Versatile applications of

electrochemical flow-through systems in water treatment processes[J]. Chemical Engineering Journal, 2023, 473: 145400.

[87] Jiang Z, Yang M, Wang Q, et al. Magnetic-assisted strategy for performance enhancement of flow-by capacitive deionization[J]. Desalination, 2023, 548: 116274.

[88] Chen R, Liu X, Wang M, et al. A novel two-stage continuous capacitive deionization system with connected flow electrode and freestanding electrode[J]. Chemical Engineering Journal, 2024, 491: 152133.

[89] Qin H, Fang F, Mao Y, et al. Insights on CDI parametric controls and dependencies using global sensitivity analysis[J]. Separation and Purification Technology, 2025, 354: 129424.

[90] Zhu Y, Miller C, Lian B, et al. Brackish groundwater desalination by constant current membrane capacitive deionization (MCDI): results of a long-term field trial in central Australia[J]. Water Research, 2024, 254: 121413.

[91] Luo L, Liu T, He J, et al. Interface gypsum deposition in flow-electrode CDI treating brackish water: impacts and mechanisms[J]. Water Research, 2025, 272: 122920.

[92] Shi C, Wang H, Li A, et al. Process model for flow-electrode capacitive deionization for energy consumption estimation and system optimization[J]. Water Research, 2023, 230: 119517.

[93] Saleem M W, Ali S, Usman M, et al. Integration of capacitive deionization and forward osmosis for high water recovery and ultrapure water production: concept, modelling and performance analysis[J]. Environmental Technology, 2024, 45(28): 6136-6157.

[94] Kong X, He J, Ma J, et al. Scaling behavior of Si in capacitive deionization (CDI) systems for brackish groundwater desalination[J]. Desalination, 2024, 583: 117703.

[95] Cuong D V. Critical review of capacitive deionization: design, operation consideration and real-world environmental applications[J]. Journal of Science and Technology in Civil Engineering (JSTCE)-HUCE, 2024, 18(1): 108-129.

[96] Zhang Y, Bu X, Dong X, et al. Nanofiltration combined with membrane capacitive deionization for efficient classification and recovery salts from simulated coal chemical industrial wastewater[J]. Separation and Purification Technology, 2023, 322: 124156.

[97] Bouhadana Y, Avraham E, Soffer A, et al. Several basic and practical aspects related to electrochemical deionization of water[J]. AIChE Journal, 2010, 56(4): 1041-1052.

[98] Lee J B, Park K K, Eum H M, et al. Desalination of a thermal power plant wastewater by membrane capacitive deionization[J]. Desalination, 2006, 196(1-3): 125-134.

[99] Zhao R, Satpradit O, Rijnaarts H H M, et al. Optimization of salt adsorption rate in membrane capacitive deionization[J]. Water Research, 2013, 47(5): 1941-1952.

[100] Bao S, Xin C, Zhang Y, et al. Application of capacitive deionization in water treatment and energy recovery: a review[J]. Energies, 2023, 16(3): 1136.

[101] He Z, Miller C J, Zhu Y, et al. Membrane capacitive deionization (MCDI): a flexible and tunable technology for customized water softening[J]. Water Research, 2024, 259: 121871.

[102] Mao Y, Long S, Kuai X, et al. Statistical uncertainty quantification to augment CDI electrode design and operation optimization[J]. Chemical Engineering Journal, 2023, 469: 143825.

[103] Li C, Sun S, Wu W, et al. Kelp-derived porous carbon for capacitive deionization: trade-off effect of activation temperature[J]. Progress in Natural Science: Materials International, 2024, 34(5): 907-912.

[104] Moreno D, Nelson H, Cary G, et al. Thermodynamic evaluation of electrode storage for capacitive deionization[J]. ACS Omega, 2025, 10: 10139-10151.

[105] Kong W, Ge X, Zhang Q, et al. Ultrafast air-plasma reduction-exfoliation of graphene oxide aerogel at room temperature for capacitive deionization[J]. Carbon, 2023, 215: 118501.

[106] Xiang M, Wang N, Sun L, et al. Capacitive deionization mechanism and multiple properties of low-temperature etched porous carbon fabric with abundant surface defects[J]. Separation and Purification Technology, 2025, 354: 128667.

[107] He Z, Liu S, Lian B, et al. Optimization of constant-current operation in membrane capacitive deionization (MCDI) using variable discharging operations[J]. Water Research, 2021, 204: 117646.

[108] Luo L, He Q, Yi D, et al. Indirect charging of carbon by aqueous redox mediators contributes to the enhanced desalination performance in flow-electrode CDI[J]. Water Research, 2022, 220: 118688.

[109] Martinez J, Colán M, Catillón R, et al. Desalination using the capacitive deionization technology with graphite/AC electrodes: effect of the flow rate and electrode thickness[J]. Membranes, 2022, 12(7): 717.

[110] Landon J, Gao X, Omosebi A, et al. Emerging investigator series: local pH effects on carbon oxidation in capacitive deionization architectures[J]. Environmental Science: Water Research & Technology, 2021, 7(5): 861-869.

[111] Yu J, Jo K, Kim T, et al. Temporal and spatial distribution of pH in flow-mode capacitive deionization and membrane capacitive deionization[J]. Desalination, 2018, 439: 188-195.

[112] Jung S M, Choi J H, Kim J H. Application of capacitive deionization (CDI) technology to insulin purification process[J]. Separation and Purification Technology, 2012, 98: 31-35.

[113] Ganzi G C, Wood J H, Griffin C S. Water purification and recycling using the CDI process[J]. Environmental Progress, 1992, 11(1): 49-53.

[114] Huang X, He D, Tang W, et al. Investigation of pH-dependent phosphate removal from wastewaters by membrane capacitive deionization (MCDI)[J]. Environmental Science: Water Research & Technology, 2017, 3(5): 875-882.

[115] Jia B, Zhang W. Preparation and application of electrodes in capacitive deionization (CDI): A state-of-art review[J]. Nanoscale Research Letters, 2016, 11(1): 64.

[116] Lee J H, Bae W S, Choi J H. Electrode reactions and

adsorption/desorption performance related to the applied potential in a capacitive deionization process[J]. Desalination, 2010, 258(1-3): 159-163.

[117] Thamilselvan A, Nesaraj A, Noel M. Review on carbon-based electrode materials for application in capacitive deionization process[J]. International Journal of Environmental Science and Technology, 2016, 13(12): 2961-2976.

[118] Suss M E, Porada S, Sun X, et al. Water desalination via capacitive deionization: what is it and what can we expect from it[J]. Energy & Environmental Science, 2015, 8(8): 2296-2319.

[119] Zhang X, Zuo K, Zhang X, et al. Selective ion separation by capacitive deionization (CDI) based technologies: a state-of-the-art review[J]. Environmental Science: Water Research & Technology, 2020, 6(2): 243-257.

[120] Sun K, Tebyetekerwa M, Wang C, et al. Electrocapacitive deionization: mechanisms, electrodes, and cell designs[J]. Advanced Functional Materials, 2023, 33(18): 2213578.

[121] Lado J J, Pérez-Roa R E, Wouters J J, et al. Evaluation of operational parameters for a capacitive deionization reactor employing asymmetric electrodes[J]. Separation and Purification Technology, 2014, 133: 236-245.

[122] Liu Y, Nie C, Liu X, et al. Review on carbon-based composite materials for capacitive deionization[J]. RSC Advances, 2015, 5(20): 15205-15225.

[123] Hou C H, Liu N L, Hsi H C. Highly porous activated carbons from resource-recovered Leucaena leucocephala wood as capacitive deionization electrodes[J]. Chemosphere, 2015, 141: 71-79.

[124] Li P I, Chen L C, Hou C H, et al. Effects of activated carbon characteristics on the electrosorption capacity of titanium dioxide/activated carbon composite electrode materials prepared by a microwave-assisted ionothermal synthesis method[J]. Journal of Colloid and Interface Science, 2015, 446: 352-358.

[125] Ratajczak P, Suss M E, Kaasik F, et al. Carbon electrodes for capacitive technologies[J]. Energy Storage Materials, 2019, 16: 126-145.

[126] Jiang Y, Alhassan S I, Wei D, et al. A review of battery materials as CDI electrodes for desalination[J]. Water, 2020, 12(11): 3030.

[127] Huang M R, Rao L, Chen J, et al. Advancements in electrode materials: the role of MXenes in capacitive deionization technology[J]. ACS Materials Letters, 2025, 7: 1400-1418.

[128] Jiang Y X, Zhang W C, Deng Y M, et al. The electrode materials in flow-electrode capacitive deionization desalination: a mini review[J]. Rare Metals, 2025, 1-20.

[129] Hu S, Fang D, Li F, et al. Recent advances in electrode materials for typical halogen removal via capacitive deionization[J]. Desalination, 2025, 601: 118608.

[130] Zhu A H, Li Y Q, Xue M, et al. The research progress on the removal of heavy metals using carbon electrodes in capacitive deionization technology[J]. Reviews in Inorganic Chemistry, 2025.

[131] Zhang M, Lu X, Kong W, et al. Hollow carbon nanocone arrays on carbon fiber cloth as a free-standing electrode for high-performance capacitive deionization[J]. Separation and Purification Technology, 2025, 359: 130771.

[132] Reinhard A G, Mehregan M, Young M J, et al. Conformal nanoscale conductive polymer films on carbon nanotube forests for electrochemical water desalination[J]. ACS Applied Nano Materials, 2025, 13: 6267-6273.

[133] Liang Y, Song Y, Sun Y, et al. Research on the desalination kinetics of carbon tableting electrodes for capacitive deionization water purification[J]. Scientific Reports, 2025, 15(1): 10837.

[134] Shahzad T, Nawaz S, Jamal H, et al. A review on cutting-edge three-dimensional graphene-based composite materials: redefining wastewater remediation for a cleaner and sustainable world[J]. Journal of Composites Science, 2025, 9(1): 18.

[135] Sahoo P K, Das S, Rao Y S, et al. Applications of solid waste-derived carbon nanomaterials in water purification[J]. Waste Derived Carbon Nanomaterials, 2025, 2: 55-83.

[136] Al-Hamadani S M, Kyaw H H, Myint M T Z, et al. Mesoporous conductive activated carbon derived from mesquite tree for capacitive deionization[J]. Biomass Conversion and Biorefinery, 2025, 1-17.

[137] Jiang D, Xu R, Bai L, et al. Insights into electrochemical paradigms for lithium extraction: electrodialysis versus capacitive deionization[J]. Coordination Chemistry Reviews, 2024, 516: 215923.

[138] Meng F, Liu Y, Ding Z, et al. Hydrogen-bonded organic framework derived 2D N, O co-doped carbon nanobelt with tunable pseudocapacitive contribution for efficient capacitive deionization[J]. Small, 2024, 20(21): 2309353.

[139] Patel S K, Ritt C L, Deshmukh A, Wang Z, Qin M, Epsztein R, Elimelech M. The relative insignificance of advanced materials in enhancing the energy efficiency of desalination technologies[J]. Energy & Environmental Science, 2020, 13(6): 1694-1710.

[140] Jin J, Xi W, Li Z, et al. Recent advances of 2D materials in capacitive deionization[J]. Desalination, 2024, 578: 117468.

[141] Moronshing M, Subramaniam C. Scalable approach to highly efficient and rapid capacitive deionization with CNT-thread as electrodes[J]. ACS Applied Materials & Interfaces, 2017, 9(46): 39907-39915.

[142] Toledo-Carrillo E, Zhang X, Laxman K, et al. Asymmetric electrode capacitive deionization for energy efficient desalination[J]. Electrochimica Acta, 2020, 358: 136939.

[143] Tian S, Wu J, Zhang X, et al. Capacitive deionization with nitrogen-doped highly ordered mesoporous carbon electrodes[J]. Chemical Engineering Journal, 2020, 380: 122514.

[144] Hui B, Zhou H, Liu A, et al. Nitrogen-rich self-doping modified porous carbon material as a CDI electrode for brine desalination[J]. Carbon Letters, 2025, 1-14.

[145] Cen B, Yang R, Li K, et al. Large capacity and rapid rate of ion removal from synthetic municipal wastewater via CDI using chitosan-based nitrogen-doped porous carbon electrode[J]. Process Safety and Environmental Protection, 2021, 147: 857-865.

[146] Shi P F, Wang C, Sun J Y, et al. Thermal conversion of

polypyrrole nanotubes to nitrogen-doped carbon nanotubes for efficient water desalination using membrane capacitive deionization[J]. Separation and Purification Technology, 2020, 235: 116196.

[147] Rana M, Santos C, Monreal-Bernal A, Vilatela J J. CNT Fiber-Based Hybrids: Synthesis, Characterization, and Applications in Energy Management[M]. In: Synthesis and Applications of Nanocarbons, 2020: 149-200.

[148] Hou C H, Liu N L, Hsu H L, et al. Development of multi-walled carbon nanotube/poly (vinyl alcohol) composite as electrode for capacitive deionization[J]. Separation and Purification Technology, 2014, 130: 7-14.

[149] Lee M Y, Kim H, Kim J O, et al. Three-dimensional hollow fiber type of carbon nanotube electrode for enhanced ion adsorption capacity[J]. Desalination and Water Treatment, 2017, 90: 46-53.

[150] Liu Z, Wei B, Liu K, et al. DBS^--doped polypyrrole/CNTs with 3D conductive architecture connected with MoS_2 as symmetrical electrodes for boosted CDI capability[J]. Separation and Purification Technology, 2024, 345: 127380.

[151] Abdelkader A, Fray D. Controlled electrochemical doping of graphene-based 3D nanoarchitecture electrodes for supercapacitors and capacitive deionisation[J]. Nanoscale, 2017, 9(38): 14548-14557.

[152] A H W, A W S, A Y L, et al. Large-scale chemical vapor deposition synthesis of graphene nanoribbions/carbon nanotubes composited for enhanced membrane capacitive deionization[J]. Journal of Electroanalytical Chemistry, 2021, 904: 115907.

[153] Li J, Ji B, Jiang R, et al. Hierarchical hole-enhanced 3D graphene assembly for highly efficient capacitive deionization[J]. Carbon, 2018, 129: 95-103.

[154] Li Z, Song B, Wu Z, et al. 3D porous graphene with ultrahigh surface area for microscale capacitive deionization[J]. Nano Energy, 2015, 11: 711-718.

[155] Liu Q, Tan G, Lei Y, et al. 3D interconnected porous graphene architecture as a high-performance capacitive deionization electrode[J]. Separation and Purification Technology, 2024, 336: 126300.

[156] Liu K, Cui J, Feng A, et al. Pore optimization engineering for enhancing ion storage and capacitive deionization properties of graphene[J]. Separation and Purification Technology, 2025, 362: 131778.

[157] Kong W, Ge X, Lu X, et al. The simpler the better: ultrafast air-plasma synthesis of 3D crosslinked graphene nanoscroll-nanosheet aerogels at room temperature for capacitive deionization[J]. Small, 2024, 20(38): 2402057.

[158] Cao J, Wang Y, Chen C, et al. A comparison of graphene hydrogels modified with single-walled/multi-walled carbon nanotubes as electrode materials for capacitive deionization[J]. Journal of Colloid and Interface Science, 2018, 518: 69-75.

[159] Qiang H, Shi M, Lu K, et al. Green self-templated synthesis of P-doped mesoporous carbon from dual sodium salts with improved average pore size for capacitive deionization[J]. Desalination, 2025, 593: 118246.

[160] Younes H, Lou D, Mao M, et al. A review on capacitive deionization: recent advances in Prussian blue analogues and carbon materials based electrodes[J]. Hybrid Advances, 2024, 6: 100191.

[161] Askari M, Rajabzadeh S, Tijing L, et al. Advances in capacitive deionization (CDI) systems for nutrient recovery from wastewater: paving the path towards a circular economy[J]. Desalination, 2024, 583: 117695.

[162] Luo G, Gao L, Zhang D, et al. Highly efficient capacitive deionization electrodes from electrospun carbon nanofiber membrane containing reduced graphene oxide and carbon nanotub[J]. Desalination and Water Treatment, 2018, 135: 157-166.

[163] Kang D, Huang C, Ding M, et al. Review on the polymer materials for capacitive deionization[J]. Desalination, 2024, 586: 117884.

[164] Zhang H, Wang Q, Li L, et al. Electric double layer capacitive adsorption and faradaic pseudo-capacitance behavior of ZnFe-PANI/CNT electrode for phosphate removal in capacitive deionization[J]. Separation and Purification Technology, 2024, 333: 125913.

[165] Zhang L, Cai Y, Fang R, et al. Construction of fully coated polypyrrole oxygen-barrier film based on MXene nanosheets for high reliability capacitive deionization[J]. Separation and Purification Technology, 2024, 337: 126362.

[166] Yang D, Wang L, Li Y, et al. Pseudocapacitive deionization of high concentrations of hexavalent chromium using NiFe-layered double hydroxide/polypyrrole asymmetric electrode[J]. Separation and Purification Technology, 2024, 328: 125004.

[167] Nie L, Ren Y, Wang L, et al. Design of polypyrrole layer enhanced MIL-88B (Fe) composite electrode material for electrosorption separation of copper ions[J]. Desalination, 2025, 603: 118606.

[168] Zhao X, Chen D, Shi M, et al. Anchoring chitosan/phytic acid complexes on polypyrrole nanotubes as capacitive deionization electrodes for uranium capture from wastewater[J]. International Journal of Biological Macromolecules, 2024, 270: 132491.

[169] Hu Y, Luo Q, Du X, et al. Film electrode by incorporating polypyrrole/carbon black into cross-linked binders of chitosan/cationic polyacrylamide for selective chloride extraction in wastewater[J]. Separation and Purification Technology, 2024, 330: 125434.

[170] Zhang Y J, Xue J Q, Li F, et al. Preparation of polypyrrole/chitosan/carbon nanotube composite nano-electrode and application to capacitive deionization process for removing Cu^{2+}[J]. Chemical Engineering and Processing, 2019, 139: 121-129.

[171] Fang R, Zhang L, Huang S, et al. 3D heterostructure constructed by ion-doped polypyrrole coupled with MoS_2@HCS and its highly efficient deionization performance[J]. Separation and Purification Technology, 2024, 339: 126606.

[172] Kong L, Chen L, Palacios E, et al. Understanding the mechanisms in lithium-ion selectivity enhancement by coating cation exchange membranes with doped polypyrrole[J]. Desalination, 2025, 609: 118857.

[173] Shehzad H, Chen J, Shuang M T, et al. Evaluation of templated N/P co-doped hierarchical mesoporous biocarbon/2D-molybdenum disulfide/polypyrrole composite as a supercapacitor electrode for U (VI) electrosorption[J]. Separation and Purification Technology, 2024, 329: 125226.

[174] Ma D, Wang Y, Han X, et al. Electrode configuration optimization of capacitive deionization cells based on zero charge potential of the electrodes[J]. Separation and Purification Technology, 2017, 189: 467-474.

[175] Wang S, Du S, Lei Y, et al. Synergistic chemical traction and pre-intercalation strategies enable high-quality MnO_2 composites for efficient ammonium capture[J]. Chemical Engineering Journal, 2024, 500: 157248.

[176] Kong W, Zhang Q, Lu X, et al. Polyaniline modified exfoliated graphene aerogel as high-performance anion-capture electrode for hybrid capacitive deionization[J]. Diamond and Related Materials, 2024, 148: 111383.

[177] Luo K, Hu T, Xing W, et al. Polyaniline/activated carbon composite based flowing electrodes for highly efficient water desalination with single-cycle operational mode[J]. Chemical Engineering Journal, 2024, 481: 148454.

[178] Wang C, Xue S, Xu Y, et al. Novel electrocatalytic capacitive deionization with catalytic electrodes for selective phosphonate degradation: performance and mechanism[J]. Water Research, 2024, 256: 121614.

[179] Zhang H, Wang Q, Liu J, et al. Deciphering heterojunction layered double hydroxide-polyaniline-carbon nanotubes for phosphorus capture in capacitive deionization[J]. Science of The Total Environment, 2024, 954: 176382.

[180] Liu F, Pignatello J J, Sun R, et al. A comprehensive review of novel adsorbents for per-and polyfluoroalkyl substances in water[J]. ACS ES& T Water, 2024, 4(4): 1191-1205.

[181] Abumadi F A, Koujan M, Laoui T, et al. Processing of carbon nanofibers with graphene oxide and carbon nanotubes additives and its application in CDI electrode material[J]. Advances in Science and Technology, 2023, 129: 13-18.

[182] Pang T, Marken F, Mattia D, et al. Advances and challenges in capacitive deionization: materials, architectures, and selective ion removal[J]. Desalination, 2024, 592: 118140.

[183] Li M, Zhao X, Xu Y, et al. A mini-review about overcoming challenges in hydrophilicity: towards efficient capacitive deionization electrodes[J]. Separation and Purification Technology, 2024, 354: 129211.

[184] Saffarimiandoab F, Sabetvand R, Zhang X. Molecular insights into capacitive deionization mechanisms inside hydrophobic and hydrophilic carbon nanotube channel electrodes[J]. Journal of Materials Chemistry A, 2022, 10(43): 23332-23340.

[185] Ma D, Wang Y, Cai Y, et al. Multifunctional group sulfobutyl ether β-cyclodextrin polymer treated CNT as the cathode for enhanced performance in asymmetric capacitive deionization[J]. Electrochimica Acta, 2019, 313: 321-330.

[186] Tao Y, Cui Y, Wang H, et al. High-efficiency electrochemical desalination: the role of a rigid pseudocapacitive polymer electrode with diverse active sites[J]. Advanced Functional Materials, 2025, 35(6): 2414805.

[187] N'Diaye J, Bagchi R, Howe J Y, et al. Redox active organic-carbon composites for capacitive electrodes: a review[J]. Sustainable Chemistry, 2021, 2(3): 407-440.

[188] Jordan J W, Townsend W J, Johnson L R, et al. Electrochemistry of redox-active molecules confined within narrow carbon nanotubes[J]. Chemical Society Reviews, 2021, 50(19): 10895-10916.

[189] Rethinasabapathy M, Bhaskaran G, Hwang S K, et al. Efficient lithium extraction using redox-active prussian blue nanoparticles-anchored activated carbon intercalation electrodes via membrane capacitive deionization[J]. Chemosphere, 2023, 336: 139256.

[190] Rauer S B, Wang S, Köller N, et al. PEDOT: PSS-CNT composite particles overcome contact resistances in slurry electrodes for flow-electrode capacitive deionization[J]. Advanced Functional Materials, 2023, 33(38): 2303606.

[191] Du R, Zhao Q, Zhang N, et al. Macroscopic carbon nanotube-based 3D monoliths[J]. Small, 2015, 11(27): 3263-3289.

[192] Min C, Zou X, Yang Q, et al. Near-infrared light responsive polymeric nanocomposites for cancer therapy[J]. Current Topics in Medicinal Chemistry, 2017, 17(16): 1805-1814.

[193] Tan R Y H, Lee C S, Pichika M R, et al. pH responsive polyurethane for the advancement of biomedical and drug delivery[J]. Polymers, 2022, 14(9): 1672.

[194] Yang S, Liu J, Ping Y, et al. Multi-functionalized single-walled carbon nanotubes as delivery carriers: promote the targeting uptake and antitumor efficacy of doxorubicin[J]. Journal of Inclusion Phenomena and Macrocyclic Chemistry, 2022, 102(9): 801-817.

[195] Xiong S, Ren L, Zhang C, et al. Block copolymer coated carbon nanotube membrane anodes for enhanced and multipurpose hybrid capacitive deionization[J]. Desalination, 2021, 520: 115368.

[196] Kou J, Wang Z, Li M, et al. Eco-friendly synthesis of TiO_2 nanoparticles for improved uranium adsorption in CDI systems[J]. Journal of Environmental Chemical Engineering, 2025, 13(1): 115230.

[197] Yuan Y L, Lu Y D, Jia B E, et al. Integrated system of solar cells with hierarchical $NiCo_2O_4$ battery-supercapacitor hybrid devices for self-driving light-emitting diodes[J]. Nano-Micro Letters, 2019, 11(1): 42.

[198] Yuan Y L, Wu Y H, Zhang T, et al. Integration of solar cells with hierarchical CoS_x nanonets hybrid supercapacitors for self-powered photodetection systems[J]. Journal of Power Sources, 2018, 404: 118-125.

[199] Yang J, Yuan Y L, Wang W C, et al. Interconnected $Co_{0.85}Se$ nanosheets as cathode materials for asymmetric

supercapacitors[J]. Journal of Power Sources, 2017, 340: 6-13.

[200] Trang N T T, Nam P T, Thom N T, et al. TiO_2-embedded 3D porous activated carbon from waste-sugarcane-bagasse: a revolutionary electrode material for unmatched desalination performance in capacitive deionization[J]. Journal of Applied Electrochemistry, 2025, 7: 1835-1848.

[201] Tang H C, Xia K Q, Lu J G, et al. $NiTe_2$-based electrochemical capacitors with high-capacitance AC line filtering for regulating TENGs to steadily drive LEDs[J]. Nano Energy, 2021, 84: 105931.

[202] Feng J, Xiong S, Ren L, et al. Atomic layer deposition of TiO_2 on carbon-nanotubes membrane for capacitive deionization removal of chromium from water[J]. Chinese Journal of Chemical Engineering, 2022, 45: 15-21.

[203] Nguyen T T L, Nguyen T T, Nguyen H A, et al. Fabrication of TiO_2/CNTs composite electrode with improved performance in capacitive deionization[J]. CLEAN-Soil, Air, Water, 2024, 52(5): 2300037.

[204] Ma S, Liu C, Xu Y, et al. TiO_2 and carbon nanotubes composites modify capacitive deionization anodes to improve the dechlorination efficiency in desulfurization wastewater[J]. Water Science and Technology, 2021, 5: 1228-1244.

[205] Gu X, Wang R, Yang S, Shangguan Y, Feng X, Chen H. Boosting capacitive deionization in MoS_2 via interfacial coordination bonding and intercalation-induced spacing confinement[J]. ACS Nano, 2025, 19(6): 6488-6498.

[206] Cai Y, Zhang W, Fang R, et al. Well-dispersed few-layered MoS_2 connected with robust 3D conductive architecture for rapid capacitive deionization process and its specific ion selectivity[J]. Desalination, 2021, 520: 115325.

[207] Dixit F, Zimmermann K, Dutta R, et al. Application of MXenes for water treatment and energy-efficient desalination: a review[J]. Journal of Hazardous Materials, 2022, 423: 127050.

[208] Zargar S A, Dehghani M A M, Soroush E, et al. Synthesis of novel 2D/2D $Ti_3C_2T_x$ MXene/1T-MoS_2 heterostructure enhanced with carbon nanotubes as a highly-efficient electrode for hybrid capacitive deionization[J]. Journal of Alloys and Compounds, 2024, 981: 173765.

[209] Siriwardane I, Rathuwadu N, Dahanayake D, et al. Nano-manganese oxide and reduced graphene oxide-incorporated polyacrylonitrile fiber mats as an electrode material for capacitive deionization (CDI) technology[J]. Nanoscale Advances, 2021, 3(9): 2585-2597.

[210] Xu S, Wang T, Wang C F, et al. The effect of crystal phase of manganese oxide on the capacitive deionization of simple electrolytes[J]. Science of the Total Environment, 2019, 675: 31-40.

[211] Shi W, Zhou X, Li J, et al. High-performance capacitive deionization via manganese oxide-coated, vertically aligned carbon nanotubes[J]. Environmental Science & Technology Letters, 2018, 5(11): 692-700.

[212] Zhao Y, Zhang L, Huang S, Fang R, Zhang S, Wang Y. Oxygen vacancy enhancing intrinsic conductivity of rGO@MnO_{2-x} electrode for efficient hybrid capacitive deionization[J]. Journal of Environmental Chemical Engineering, 2024, 12(1): 111883.

[213] Nguyen H A, Le T T L, To M D, et al. Preparation of layered structure MnO_2/CNTs composites for high-performance salt removal by hybrid capacitive deionization[J]. Journal of Solid State Electrochemistry, 2024, 28(10): 3961-3972.

[214] Liu Y, Zhou L, Ouyang J, et al. Electrodeposition nanofabrication of carboxylated carbon nanotubes/α-MnO_2 nanorods/polypyrrole composites as high hybrid capacitance electrodes for efficient U (VI) electrosorption[J]. Separation and Purification Technology, 2024, 334: 125989.

[215] Wang S, Wang G, Wang X, et al. Enhancing the capacitive deionization performance of $NaMnO_2$ by interface engineering and redox-reaction[J]. Environmental Science: Nano, 2019, 6(8): 2379-2388.

[216] Wadi V S, Ibrahim Y, Arangadi A F, et al. Three-dimensional graphene/MWCNT-MnO_2 nanocomposites for high-performance capacitive deionization (CDI) application[J]. Journal of Electroanalytical Chemistry, 2022, 914: 116318.

[217] Sun J, Li Y, Song H, et al. Enhanced capacitive deionization properties of activated carbon doped with carbon nanotube-bridged molybdenum disulfide[J]. Chemosphere, 2023, 310: 136740.

[218] Huynh L T N, Nguyen H A, Pham H V, et al. Electrosorption of Cu (II) and Zn (II) in capacitive deionization by KOH activation coconut-shell activated carbon[J]. Arabian Journal for Science and Engineering, 2023, 48(1): 551-560.

[219] Hussain H, Jilani A, Salah N, et al. Freestanding activated carbon nanocomposite electrodes for capacitive deionization of water[J]. Polymers, 2022, 14(14): 2891.

[220] Wang W, Li K, Song G, Zhou M, Tan P. Activated carbon aerogel as an electrode with high specific capacitance for capacitive deionization[J]. Processes, 2022, 10(12): 2670.

[221] Zhu G, Wang W, Li X, et al. Design and fabrication of a graphene/carbon nanotubes/activated carbon hybrid and its application for capacitive deionization[J]. RSC Advances, 2016, 6(7): 5817-5823.

[222] Xie J, Ma J, Wu L, et al. Carbon nanotubes in-situ cross-linking the activated carbon electrode for high-performance capacitive deionization[J]. Separation and Purification Technology, 2020, 239: 116593.

[223] Chand H, Liu Z, Wei Q, et al. Performance and mechanism of chromium removal using flow electrode capacitive deionization (FCDI): validation and optimization[J]. Separation and Purification Technology, 2024, 340: 126696.

[224] Hellen S, Mlsna T E, Wipf D O. Functionalized biochar electrodes for asymmetrical capacitive deionization[J]. Desalination, 2021, 516: 115240.

[225] Cuong D V, Wu P C, Liu N L, et al. Hierarchical porous carbon derived from activated biochar as an eco-friendly electrode for the electrosorption of inorganic ions[J]. Separation and Purification

Technology, 2020, 242: 116813.

[226] Jinitha C G, Abisha P, Sonia S, et al. A critical review of activated carbon for CDI electrodes, emphasizing its biomass and commercial sources, activation methods, performance analysis, and future advancements[J]. Biomass Conversion and Biorefinery, 2025, 15(11): 16273-16306.

[227] Wang Y, Chen D, Xue X, et al. Surface functionalized biochar for the effective capacitive deionization of lead ions[J]. Separation and Purification Technology, 2024, 350: 127907.

[228] Jiang J J, Ma X J, Zhou J, et al. Biomass-derived carbons and their modification techniques in electrochemical capacitive deionization desalination[J]. RSC Sustainability, 2025.

[229] Nguyen T T, Pham T N, Tran T N, et al. Enhanced capacitive deionization performance of activated carbon derived from coconut shell electrodes with low content carbon nanotubes-graphene synergistic hybrid additive[J]. Materials Letters, 2021, 292: 129652.

[230] Huang Z H, Yang Z, Kang F, et al. Carbon electrodes for capacitive deionization[J]. Journal of Materials Chemistry A, 2017, 5(2): 470-496.

[231] Liu L, Liao L, Meng Q, Cao B. High performance graphene composite microsphere electrodes for capacitive deionisation[J]. Carbon, 2015, 90: 75-84.

[232] Lee B, Park N, Kang K S, et al. Enhanced capacitive deionization by dispersion of CNTs in activated carbon electrode[J]. ACS Sustainable Chemistry & Engineering, 2018, 6(2): 1572-1579.

[233] Ezzati M, Hekmat F, Shahrokhian S, et al. Titanium disulfide decorated hollow carbon spheres towards capacitive deionization[J]. Desalination, 2022, 533: 115766.

[234] Cheng Y T, Hao Z Q, Hao C R, et al. A review of modification of carbon electrode material in capacitive deionization[J]. RSC Advances, 2019, 9(42): 24401-24419.

[235] Cai Y M, Zhao F, Zhao J S, et al. Flexible construction of three-dimensional continuous conductive structure by hollow carbon sphere and CNT for promoted ions transport in flow-electrode capacitive deionization[J]. Separation and Purification Technology, 2024, 337: 126405.

[236] Zhang Y, Wu J Y, Zhang S H, et al. MOF-on-MOF nanoarchitectures for selectively functionalized nitrogen-doped carbon-graphitic carbon/carbon nanotubes heterostructure with high capacitive deionization performance[J]. Nano Energy, 2022, 97: 107146.

[237] Ngo Minh P, Nguyen Anh Thu T, Tran Minh K, et al. ZIF-67 metal-organic frameworks and CNTs-derived nanoporous carbon structures as novel electrodes for flow-electrode capacitive deionization[J]. Separation and Purification Technology, 2021, 277: 119466.

[238] Lim J H, Lee H C, Lee S K, et al. Capacitive deionization incorporating a fluidic MOF-CNT electrode for the high selective extraction of lithium[J]. Desalination, 2024, 578: 117403.

[239] Khan M S, Leong Z Y, Li D S, et al. A mini review on metal-organic framework-based electrode materials for capacitive deionization[J]. Nanoscale, 2023, 15(39): 15929-15949.

[240] Rangaraj V M, Yoo J I, Song J K, et al. MOF-derived 3D MnO_2@ graphene/CNT and Ag@ graphene/CNT hybrid electrode materials for dual-ion selective pseudocapacitive deionization[J]. Desalination, 2023, 550: 116369.

[241] Qian H F, Yang J M, Hu B, et al. Partially reduced CeO_2/C@CNT with high oxygen vacancy boosting phosphate adsorption as CDI anode[J]. Separation and Purification Technology, 2023, 306: 122557.

[242] Ngo Minh P, Jung E, Nguyen Anh Thu T, et al. Enhanced desalination performance of capacitive deionization using nanoporous carbon derived from ZIF-67 metal organic frameworks and CNTs[J]. Nanomaterials, 2020, 10(11): 2091.

[243] Akulwar M, Bailmare D B, Jugade R M, et al. Tailoring iron MOF/carbon nanotube composites as flow electrodes for high-performance capacitive deionization[J]. Discover Materials, 2024, 4(1): 54.